Energy, Mines and Resources Canada
Énergie, Mines et Ressources Canada

CANMET
Canada Centre for Mineral and Energy Technology
Centre canadien de la technologie des minéraux et de l'énergie

CATALYSIS, MOLECULAR WEIGHT CHANGE, AND FOSSIL FUELS

MARTEN TERNAN,
HYDROCARBON PROCESSING RESEARCH LABORATORY

JANUARY 1983

ENERGY RESEARCH PROGRAM
ENERGY RESEARCH LABORATORIES
REPORT ERP/ERL 83-03 (J)

CATALYSIS, MOLECULAR WEIGHT CHANGE AND FOSSIL FUELS

by

Marten Ternan
Energy Research Laboratories,
Department of Energy, Mines and Resources,
Ottawa, Ontario. K1A 0G1 Canada

The material presented here describes the author's current views on the way catalysts cause changes in the molecular weight of carbonaceous molecules in fossil fuels. Three examples have been chosen, hydrocracking residua (molecules boiling above +525°C) and heavy gas oil, gasifying char (via the carbon-steam reaction), and converting natural gas to distillate liquids. The first two examples produce decreases in molecular weight, the third an increase. Greater emphasis has been given to hydrocracking since the author has had more exposure to that topic.

HYDROCRACKING

As the amount of conventional petroleum crude oil which can be produced in Canada decreases, interest in residual hydrocarbon feedstocks rises. There are at least three different sources of residua:

1. conventional petroleum residuum (the pitch fraction which nominally boils above 525°C);
2. bitumen derived from Oil Sands (approximately 50 mass percent boils above 525°C); and
3. heavy crude oils (they contain a higher proportion of +525°C pitch than conventional crude oils).

CATALYSIS, MOLECULAR WEIGHT CHANGE AND FOSSIL FUELS[1]

by

Marten Ternan
Energy Research Laboratories,
Department of Energy, Mines and Resources,
Ottawa, Ontario. K1A 0G1 Canada

ABSTRACT

Hydrocracking and gasification are processes which decrease the molecular weight of fossil fuel feedstocks. The conversion of natural gas to hydrocarbon liquids involves an increase in molecular weight. The reaction sites of the catalysts used to accomplish these molecular weight changes are described. Since changes in the valence electrons are responsible for the cleavage and formation of the chemical bonds in hydrocarbon molecules, the solid catalyst has also been described in terms of its electronic characteristics. The description of a catalyst in these terms is able to provide a qualitative explanation for its function in molecular weight change reactions. Changes in conversion caused by variations in catalyst composition are also explained.

---

[1] ERCO Award Lecture, presented October 8, 1981 at the Second World Congress of Chemical Engineering, Montreal, Canada.

CATALYSIS, MOLECULAR WEIGHT CHANGE AND FOSSIL FUELS

by

Marten Ternan
Energy Research Laboratories,
Department of Energy, Mines and Resources,
Ottawa, Ontario. K1A 0G1 Canada

The material presented here describes the author's current views on the way catalysts cause changes in the molecular weight of carbonaceous molecules in fossil fuels. Three examples have been chosen, hydrocracking residua (molecules boiling above +525°C) and heavy gas oil, gasifying char (via the carbon-steam reaction), and converting natural gas to distillate liquids. The first two examples produce decreases in molecular weight, the third an increase. Greater emphasis has been given to hydrocracking since the author has had more exposure to that topic.

HYDROCRACKING

As the amount of conventional petroleum crude oil which can be produced in Canada decreases, interest in residual hydrocarbon feedstocks rises. There are at least three different sources of residua:

1. conventional petroleum residuum (the pitch fraction which nominally boils above 525°C);
2. bitumen derived from Oil Sands (approximately 50 mass percent boils above 525°C); and
3. heavy crude oils (they contain a higher proportion of +525°C pitch than conventional crude oils).

In each case, the object is to convert the large pitch molecules into smaller ones which can be used in distillate fuels.

There are two basic approaches. Coking processes([1],[2]) utilize pyrolysis reactions to produce distillable oils plus a coke by-product. Often large quantities of the coke by-product, containing substantial amounts of heteroatoms (e.g. sulphur, vanadium), are produced. Alternatively, hydrocracking processes utilize a combination of pyrolysis reactions and hydrogenation reactions to produce higher yields of distillable oils without producing large quantities of by-product coke. The greater costs of additional hydrogen and high pressure equipment required in hydrocracking processes must be offset by the improved quality of the oil and by the additional revenue from the higher oil yield.

Hydrocracking processes may be divided into two types: the first type utilizes a relatively high cost catalyst [typically cobalt (or nickel) and molybdenum sulphides on a gamma alumina support]. This type of catalyst has been used in commercial plants([3]) for hydrocracking residua to lower molecular weight hydrocarbons. In addition, several commercial catalytic hydrocracking units have been built to desulphurize residua without major changes in hydrocarbon molecular weight. As the catalyst time-on-stream increases, the catalyst is deactivated by the deposition of carbonaceous material, metals from organometallic compounds in the feedstock, and clay or sand in the feedstock.

The second type of hydrocracking process uses a disposable catalyst. An example would be the CANMET Hydrocracking process (4, 5). In this case a low-cost catalyst is discarded after being used once. The deposition of carbonaceous material, metals and clay on this catalyst is of little concern since the catalyst is not being used again. The present discussion will refer to the catalysts employed in the first type of residuum hydrocracking process. Most of the reaction data presented were obtained either with bitumen from the Athabasca Oil Sands or heavy gas oil derived from the bitumen.

Reactions and Reaction Sites

Several types of reactions occur on hydrocracking catalysts. Figure 1 shows some examples of hydrodesulphurization, hydrodeoxygenation, hydrodenitrogenation, hydrodemetallization, and molecular weight reduction (hydrogenation and bond cleavage) reactions. All of the above are desirable hydrocracking reactions, and they can be generalized as in Equation 1:

$$\text{Carbonaceous Molecule} + \text{Hydrogen} \longrightarrow \text{Reaction Products} \qquad (1)$$

There has been considerable work reported in the literature describing hydrodesulphurization (6-12), hydrodeoxygenation (13), hydrodenitrogenation (14-17), hydrodemetallization (18) and hydrogenation (19-23) - of pure compounds having three or more aromatic rings. Other reactions which occur on hydrocracking catalysts include polymerization, Equation 2:

$$nR \longrightarrow R_1\text{-}R_2\text{-}\ldots\text{-}R_n \text{ (i.e. Coke)} \qquad (2)$$

and dehydrogenation, Equation 3. If the reaction temperature becomes too high,

$$R_1H\text{-}R_2H \longrightarrow R_1 = R_2 + H_2 \qquad (3)$$

thermodynamic equilibrium will favor dehydrogenation rather than hydrogenation. These undesirable reactions can be generalized as in Equation 4:

$$\text{Carbonaceous Molecule} \longrightarrow \text{Reaction Products} \qquad (4)$$

Hydrogen, in Equation 1, can be considered to be chemisorbed by electron holes (represented as ⊕) in the catalyst. Wise and co-workers (24-28) have reported experimental evidence for the relationship between hydrogenation and p-conductivity of sulphided cobalt-molybdenum catalysts. They found that the introduction of sulphur anions and cobalt cations into the catalyst enhances p-conductivity (by electron holes). They concluded that hydrogen atoms were chemisorbed as protons and that this effect was promoted by the addition of sulphur anions into the catalyst (25). Wright and co-workers (29) also concluded that hydrogen is chemisorbed on sulphur anions from their inelastic neutron scattering measurements on molybdenum sulphide catalysts.

The presence of electron holes in MoS_2 is illustrated schematically in Figures 2 to 4. Stoichiometric MoS_2 is shown in Figure 2. Figure 2A shows its layer structure with a layer of Mo^{4+} between two S^{2-} layers. Figure 2B is a two-dimensional arithmetic representation (30). Figure 2C is an energy band diagram for intrinsic (no impurities) MoS_2. Values for the band gap (31, 32) and work function (33) in Figure 3 were taken from the literature.

Figure 3 shows non-stoichiometric MoS_2 containing excess sulphur anions. The excess sulphur anions will cause dislocations in the sulphur layers. This probably changes the trigonal prismatic structure (34, 35) of stoichiometric MoS_2 to a distorted octahedral structure (36) as shown in Figure 3A. For example, the molybdenum cations in MoO_3 occupy octahedral sites in the oxygen anion lattice. Figure 3B shows that the presence of each excess sulphur cation requires two additional electron holes in order to maintain electrical neutrality. Figure 3C shows the presence of electron holes in the valence band (sulphur anions) causes the Fermi level (electrochemical potential) to shift from the centre of the band gap (Figure 2C) nearer to the upper edge of the valence band.

Figure 4 shows the presence of cobalt cations in the MoS_2. In this work cobalt (shown as the cross hatched circle in Figure 4A) is considered to occupy molybdenum cation lattice positions either at the edge planes or within the bulk of MoS_2, in accordance with the views of Topsoe and co-workers (37, 38). Figure 4B shows that each cobalt cation present requires two electron holes in order to maintain electrical neutrality in the structure. Figure 4C shows that the presence of electron holes in the valence band (sulphide anions) causes the Fermi level to be located near the upper edge of the valance band.

The carbonaceous molecule in Equation 1 can be considered to be chemisorbed by electron acceptor states (represented as $\square$) in the catalyst. They are associated with catalyst sites which adsorb species as anions. They are not electron holes. Examples of electron acceptor states include anion vacancies in molybdenum sulphides and Lewis acid sites in Al_2O_3. Anion vacancies will only exist if the corresponding cation is either capable of changing its valance state (Mo^{4+} to Mo^{6+}) or has orbitals available to accomodate electrons, such as electron pair acceptors which are Lewis acid sites (Al^{3+}).

Electronic phenomena in catalysts have often been associated with solid acidity. Morrison (39) has described the similarity between the chemical concept of surface acidity and the electronic concept of surface states. Carbonaceous molecules are considered to react on acidic sites (electron acceptor states) on silica-alumina cracking catalysts. Tanabe and co-workers (40, 41) have explained surface acidity (electron acceptor states) in terms an excess charge on binary metal oxides. Heckelsberg and Banks (42) have explained catalytic cracking in terms of electron transfer which occurs via electron acceptor states.

The chemisorption of a carbonaceous molecule (CM) by electron acceptor states in gamma alumina (Al_2O_3) can be represented by Equation 5. The Al^{3+}

$$\begin{array}{c} \square \\ O^{2-}\ Al^{3+}\ O^{2+} \\ O^{2-} \end{array} + CM \longrightarrow \begin{array}{c} CM \\ O^{2-}\ Al^{3+}\ O^{2} \\ O^{2-} \end{array} \qquad (5)$$

cations are the adsorption sites. In Al_2O_3 each oxygen anion can be visualized as forming two sigma bonds, each with a different aluminum cation. These bonds are formed using two empty 2p atomic oxygen orbitals. Similarily, each alumina cation forms three sigma bonds, each with a different oxygen anion. These bonds are formed using three hybridized sp^2 atomic aluminum orbitals. There are still other empty p orbitals in the aluminum cations. For example, a fourth aluminum sigma band could form by having four hybridized sp^3 atomic orbitals. It is the ability of the aluminum anions to form additional bonds which creates electron acceptor states (or Lewis acid sites) in Al_2O_3. Of course the above explanation is over-simplified. The electronegativities indicate that the bonding is neither completely ionic (anions and cations) nor completely covalent as described above.

Gamma alumina has a spinel structure (43). The interaction of an adsorbed aromatic molecule with the alumina surface (44) is shown in Figure 5. The basis for this figure was obtained from the work of Tanabe and Nishizaki (45). The pi electrons in the aromatic molecule can interact with the electron acceptor states (Al^{3+} cations) to form the chemisorbed species. The solid hexagon represents a ring of carbon atoms in an aromatic molecule. The dotted hexagon represents the pi electrons below the carbon ring. In order to simplify the drawing the pi electrons above the carbon ring have not been shown.

Anion vacancies in molybdenum sulphides are another type of electron acceptor states. Lipsch and Schuit (46) suggested that oxygen anion vacancies in MoO_3 on Al_2O_3 were responsible for thiophene hydrodesulphurization. This concept was later extended to sulphided catalysts having a capping layer with sulphur anion vacancies (47). In a separate study, Voorhoeve and Stuiver (48) concluded that sulphur anion vacancies in tungsten sulphide catalysts were responsible for hydrogenation reactions.

There are probably no sulphur anion vacancies in MoS_2, present in sulphided cobalt-molybdenum-alumina catalysts at typical commercial operating conditions. At these conditions there will be a substantial partial pressure of H_2S formed in the hydrodesulphurization reaction with the residuum feedstock. Thermodynamic calculations have been made for the reaction shown in Equation 6:

$$MoS_2 + H_2S \longrightarrow MoS_3 + H_2 \qquad (6)$$

Thermodynamic data for standard heats of formation, standard entropies and heat capacities were taken from reference sources (49, 50). The top of Figure 6 shows the equilibrium constant plotted as a function of temperature. The mole fractions in the solid phase are represented by "x" and the mole fractions in the gas phase are represented by "y". It is apparent that the equilibrium concentration of MoS_3 in the solid phase increases with temperature. The amount of MoS_3 in the solid phase is shown in the lower part of Figure 6 as a function of the ratio of H_2S to H_2 in the gas phase. These calculations indicate that at reaction conditions the molybdenum should be present primarily as MoS_2 with a small amount of MoS_3. Actually, the amount of MoS_3 will be somewhat greater than that shown in Figure 6. All of the sulphur containing hydrocarbon species in the reactor will react with MoS_2 in a manner similar to H_2S as shown in Equation 6.

The role of the reaction centers (electron holes and electron acceptor states) can now be illustrated. The intention of this discussion is to present a description of the catalyst which will provide a qualitative understanding of reaction sites and how they are affected by changes in catalyst composition. A sulphur containing carbonaceous molecule, CM-S, which in resid hydrocracking would probably be a polycyclic aromatic molecule containing a thiophenic ring, can be used as an example. In Equation 7, the sulphur containing carbonaceous

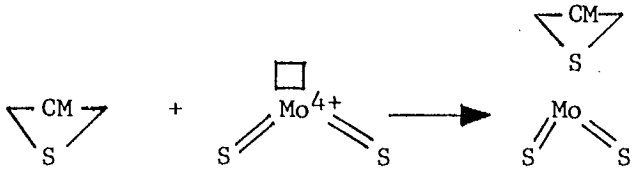

(7)

molecule, CM-S, is chemisorbed by an electron acceptor state, □, which is a sulphur vacancy in MoS_3, represented as MoS_2 in Equation 7. The chemisorbed

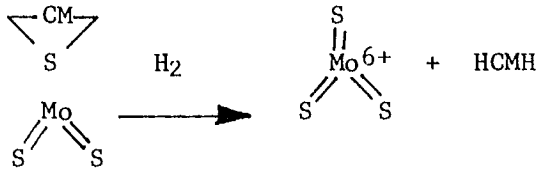

(8)

species can react with hydrogen, as shown in Equation 8. The hydrogen which reacts is also chemisorbed on the catalyst in a manner to be described below. The reaction products are MoS_3 and a carbonaceous molecule. The sulphur has been removed from the carbonaceous molecule, and the sulphur-carbon bonds have been replaced by hydrogen-carbon bonds.

The MoS_3 product can also be considered as MoS_2 containing excess non-stoichiometric sulphur. It may be preferable to consider it this way since the above thermodynamic calculations indicate that most of the molybdenum is present as MoS_2. The non-stoichiometric MoS_2 containing excess sulphur must contain electron holes in order to preserve electrical neutrality in the catalyst. This is illustrated in Equation (9), and in Figure 3B.

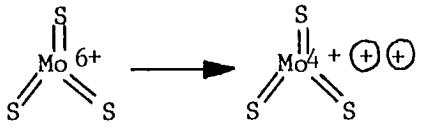

(9)

A non-stoichiometric MoS_2 species containing electron holes is probably a more realistic concept since the excess sulphur and the electron holes will probably be shared throughout the solid catalyst and not localized at a single molybdenum cation. Experimental evidence for an increase in p-conductivity (and therefore an increase in electron holes) caused by an increase catalyst sulphur content has been demonstrated by Aoshima and Wise (24).

The chemisorption of hydrogen by electron holes, as shown in Equation 10, is probably oversimplified, although Wentrcek and Wise (25) claim that

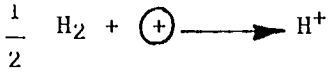

(10)

hydrogen is chemisorbed as protons. The chemisorbed protons are more likely associated with sulphur anions as shown in Equation 11.

Equation 11 is consistent with the results of Wright and co-workers (29) who found that hydrogen is chemisorbed on sulphur. In any case, both

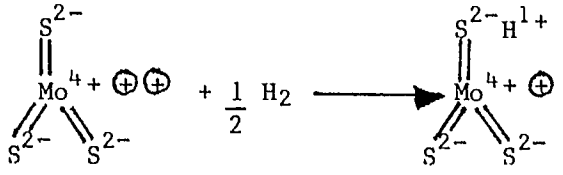

(11)

Equation 10 and 11 are consistent with hydrogen being chemisorbed by electron holes. The SH hydrogen species in Equation 11 is probably the source of hydrogen in Equation 8. Hydrogen chemisorption eventualy leads to the formation of H_2S and the regeneration of the sulphur vacancy, as shown in Equation 12.

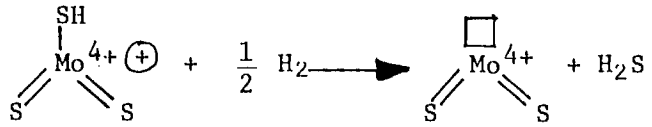

(12)

In summary, carbonaceous molecules are chemisorbed by electron acceptor states (sulphur vacancies are one example) and hydrogen is chemisorbed by electron holes. One can visualize the catalyst containing a lattice of sulphur anions which may be equally shared by all of the molybdenum (and cobalt) cations. Thus, a non-stoichiometric sulphur anion is not chemisorbed by any one single molybdenum cation. Similarly, the electron holes can move throughout the catalyst and are not localized in one particular molybdenum cation.

Equations 7 to 12 illustrate the type of catalyst reaction sites which are required for the hydrocracking process. These equations have been written with the reactant being a sulphur containing carbonaceous molecule. Similar equations can be written if the atom of the carbonaceous molecule being chemisorbed is nitrogen, oxygen, or carbon. In each case, cleavage of a sulphur-carbon, nitrogen-carbon, oxygen-carbon or carbon-carbon bond is required. Equations analogous to Equation 8 could be written for each type of bond.

In each case of carbon-carbon bond cleavage the reaction product will vary with the type of hydrocarbon reactant molecule. For paraffinic molecules, as soon as one carbon-carbon bond is broken, two different molecular fragments will be formed. Ideally, the original carbon-carbon bond will be replaced by two carbon-hydrogen bonds and both molecular species will be desorbed from the catalyst. In contrast, cleavage of a single carbon-carbon bond in an aromatic ring will not result in two molecular fragments. Nevertheless, hydrogenation of the broken carbon-carbon bond to form two carbon-hydrogen bonds is still desirable. Alternatively, one of the unsaturated carbon atoms may polymerize with another carbonaceous molecule. Such polymerization reactions can contribute to coke formation on the catalyst.

If the desirable reaction shown in Equation 1 were an elementary reaction, its rate could be expressed as in Equation 13 for the reactants, and as in Equation 14 for the catalyst reaction sites. Two site mechanisms have been

$$\text{Rate} \propto [CM][H_2] \tag{13}$$

$$\text{Rate} \propto [\square][\oplus] \tag{14}$$

proposed previously (51-53). In particular, Massoth (53) suggested the one site was for hydrogen and the other for the hydrocarbon species which he used (thiophene). Similarily, for the undesirable reaction shown in Equation 4, its rate could be shown as Equation 15 for the reactant species and Equation 16 for

$$\text{Rate} \propto [CM] \tag{15}$$

$$\text{Rate} \propto [\square] \tag{16}$$

the catalyst reaction sites. These equations indicate that desirable hydrocracking reactions are influenced by both electron acceptor states and electron holes whereas undesirable hydrocracking reactions will be primarily influenced by electron acceptor states.

The present discussion will use the hydrodesulphurization reaction as an example of a desirable hydrocracking reaction. This procedure can be justified on the basis of previous findings, that hydrodesulphurization (54), hydrodenitrogenation (54), molecular weight changes (54) and hydrogenation (55) reactions all follow similar (not identical) trends with changes in catalyst composition. The deposition of carbonaceous material on the catalyst surface will be used as an example of an undesirable hydrocracking reaction. Not all of the references cited used exactly the same experimental procedure to measure catalyst coke content. This will affect the absolute values reported, but should not influence the directional change in catalyst coke content with the variable being discussed. In each case the statistical number of coke monolayers has been calculated using the mass per cent coke on the catalyst and the catalyst surface area. It was assumed that the coke had a density of 1.2 g/mL (56) and had the same thickness as an aromatic molecule, 0.34 nm (57)

Any explanation of catalytic effects should describe both desirable and undesirable reactions. The present discussion attempts to describe the behaviour of the catalyst in both reactions.

Sulphur Effects

The presence of hydrogen sulphide is known to have an inhibiting effect on the hydrodesulphurization reaction. This phenomenon has been discussed by de Beer and co-workers (58), Broderick et al (59), Owens and Amberg (60), Hagenbach et al (61) and Vrinat et al (62). Some of the results reported in Figure 2 of Metcalfe's work (63) have been re-plotted here in Figure 7. His results clearly show that the extent of reaction decreases with increasing amount of hydrogen sulphide in the hydrogen gas contacting the catalyst.

The general phenomenon can be explained by hydrogen sulphide competing with sulphur containing carbonaceous molecules for the electron acceptor states. As an example, the sulphur vacancies in molybdenum sulphide are shown in Equation 17. Some of the electron acceptor states are occupied by sulphur

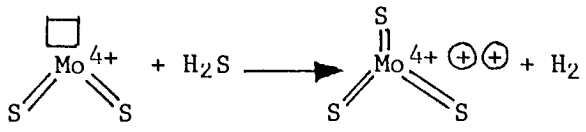

(17)

anions from H_2S, and are not available to the reactant molecule. As the amount of H_2S in the gas phase increased, the proportion of electron acceptor states occupied by sulphur anions would also increase. This would explain Metcalfe's results shown in Figure 7.

Several workers (58, 64, 65) have measured the amount of sulphur in the catalyst. Results obtained in our laboratory (64) are shown in Figure 8. The catalyst with the greatest amount of coke in Figure 8 was the one sulphided with gas oil (shown in Figure 2 of reference 64). The catalyst with the least amount of coke was the one sulphided with H_2S followed by two reaction experiments (Figure 2, reference 64). The catalyst containing the intermediate amount of coke was sulphided with H_2S followed by four reaction experiments and was described in the text of reference 64.

Figure 8 shows clearly that both sulphur conversion and catalyst coke content decrease as the amount of sulphur in the catalyst increases. The data are consistent with Equation 17. As more electron acceptor states are filled with sulphur anions, they are not available to the reactant. The lower surface concentration of carbonaceous species will decrease both sulphur conversion and coke formation. The data in Figure 8 are consistent with Equations 14 and 16, showing that both desirable and undesirable hydrocracking reactions are affected

by the concentration of electron acceptor states. In this case, filling electron acceptor states with sulphur decreases both desirable and undesirable reactions.

The arrow in Figure 8 indicates the stoichiometric amount of sulphur in the catalyst necessary for all the molybdenum and nickel to be present as MoS_2 and Ni_3S_2. This stoichiometry has been suggested by Brewer and Cheavens (66) and supported by the data of de Beer (67). Two of the catalysts in Figure 8 contain excess non-stoichiometric sulphur. Massoth et al (65) have pointed out that some workers have reported more sulphur than the stoichiometric amount. They show (65) that stoichiometric amounts of sulphur are obtained by purging with an inert gas at reaction temperature prior to the sulphur determination. This procedure removes adsorbed H_2S but not sulphides. The data in Figure 8 were obtained (64) after the reaction period by flowing hydrogen through the catalyst bed at 525°C (higher than reaction temperature) and then performing the sulphur analyses without allowing air to contact the catalyst. This procedure did produce stoichiometric values for many of the catalysts studied (64). However, the catalysts in Figure 8 definitely have excess non-stoichiometric sulphur which, according to the procedure of Massoth et al (65), should not be attributed to adsorbed H_2S. It must be emphasized that if air contacts the catalyst prior to the catalyst sulphur determination, erratic results are obtained. Observations in our laboratory were in agreement with those of de Beer et al (58), that SO_2 can be formed on exposure to air. Furthermore, Morup et al (68) have reported different Mossbauer spectra for sulphided catalysts and "air-exposed" catalysts.

Under reaction conditions the amount of sulphur in the catalyst will depend on the sulphur content of the reactor fluids (e.g. H_2S) as shown in Figure 6. Excess non-stoichiometric sulphur, as indicated in Equation 17, would probably be removed easily during a hydrogen purge (64), an inert purge (65) or exposure of the catalyst to air (58). Whether the catalyst contains excess sulphur, as in Equation 17, plus chemisorbed hydrogen, as in Equation 11, or whether the excess sulphur is present as H_2S (65), has not been resolved. Very recently X-ray photoelectron spectroscopy data (69) have been obtained on catalysts which had not been exposed to the atmosphere. They show the existence of excess non-stoichiometric sulphur, which is either adsorbed hydrogen sulphide or elemental sulphur. Thus, under reaction conditions the catalyst in its working state will contain excess non-stoichiometric sulphur. This sulphur will likely

be removed during post reaction catalyst handling and therefore not be measured in many sulphur determinations.

Molybdenum Concentration Effects

As described previously, there are at least two different types of electron acceptor states. As the proportion of the molybdenum in the MoO_3-Al_2O_3 catalyst increases, the number of molybdenum electron acceptor states, illustrated in Equation 7, will increase, and the number of alumina electron acceptor states, illustrated in Equation 5, will decrease. Reaction results obtained with this type of catalyst are shown in Figure 9. These catalysts were prepared by adding an aqueous solution of a molybdenum salt to an alumina gel. This procedure should ensure that there is intimate mixing of the molybdenum species with the colloidal particles of the alumina gel. The structure of these gels are among those discussed recently (70). After drying and calcining, the surface molybdenum composition of the catalyst is usually similar to its bulk composition (Figure 3 of reference 71). In its sulphided form, the catalyst will contain at least two phases, an oxide (alumina) phase and a sulphide phase containing molybdenum. The molybdenum sulphide phase can exist either as a surface phase (epitaxial monolayer) or as a bulk phase.

The data (54, 72) in Figure 9 show that the amount of sulphur removed increases with the molybdenum content in the catalyst. Equations 7, 8, 11 and 12 show the sequence of hydrodesulphurization reactions, which require the cleavage of the sulphur-carbon bond. Other hydrocracking reactions involving the cleavage of carbon-nitrogen, carbon-carbon bonds, etc. will occur in a somewhat similar manner. By increasing the molybdenum content of the catalyst, both the number of molybdenum electron acceptor states and the number of electron holes increase. Equation 14 shows that both electron acceptor states and electron holes are necessary for desirable hydrocracking reactions, such as sulphur removal. The increase in sulphur removal with molybdenum content in the catalyst shown in Figure 9 is therefore consistent with Equation 14. Sulphur removal increases greatly between 0 and 4 mass percent MoO_3 in the catalyst. It increases much more gradually with further increases in catalyst MoO_3 concentration. The reason for this is not known. However, it may be related to the size of the carbonaceous molecules adsorbed on the surface of the catalyst. The chemisorption bond may be formed between a single atom of a carbonaceous

molecule and a single electron acceptor state. If it is a large molecule, the rest of the molecule may geometrically cover several other electron acceptor states (reaction sites) without the formation of other chemisorptive bonds. Perhaps the number of carbonaceous molecules chemisorbed by 4 mass percent MoO_3 can prevent effective interaction of additional carbonaceous molecules with additional molybdenum electron acceptor states.

Figure 9 also shows that the amount of coke on the catalyst decreases with increasing MoO_3 in the catalyst. This can be explaind in rather simple terms or in rather elaborate terms. The simple explanation involves the decreasing number of alumina electron acceptor states and the increasing number of molybdenum electron acceptor states. The coke measured in Figure 9 was reasonably strongly bonded to the catalyst surface, since these measurements were made after the catalyst had been treated by a flowing stream of hydrogen at 525°C. If the coke was more strongly bound to the alumina than to the molybdenum, then a decrease in coke with increasing molybdenum content would be expected, as shown in Figure 9.

A more elaborate discussion is required to explain why coke is more strongly bound to alumina electron acceptor states than to molybdenum electron acceptor states. The bond is formed by the carbonaceous molecule by transferring or sharing some of its (pi) electrons with the electron acceptor sites in the catalyst. Wolkenstein (73) has described chemisorption in terms of electron sharing. As an example, the ionization potential (energy required to remove an electron from its orbital and place it at infinity) for anthracene is 7.55 eV. In the present case, the electrons of the carbonaceous molecule are being shared (not removed) with the catalyst, so the energy required to displace the electrons will be lower than the ionization potential. Furthermore, there is energy produced from the stabilization effect which results from the coordination (74) of the carbonaceous molecule with the electron acceptor state. Usually the energy produced by stabilization exceeds that required to slightly displace an electron from the carbonaceous molecule. This is why chemisorption is usually an exothermic process (75).

This argument can be seen clearly by referring to Figure 10, which represents two phases in a sulphided, Mo-Al_2O_3 catalyst. Based on Figures 2 and 5, the energy band diagrams have been drawn for intrinsic alumina and intrinsic MoS_2, that is pure alumina and pure MoS_2, without impurities. The locations of the band edges in Figure 10 are only approximations. However, they should be adequate for the present discussion. Under these conditions, the Fermi level (electrochemical potential) will be at the center of the band gap as shown in Figure 10. Descriptions of the electronic structure of solids (76) and of free molecules (77) have been given. When a single carbonaceous molecule is chemisorbed, the pi electrons (see Figure 5) will enter the conduction band. This will cause the Fermi level to move upward toward the lower edge of the conduction band. Since the Fermi level is lower in Al_2O_3 than in MoS_2, more stabilization energy will be produced in Al_2O_3. Similarly, when coke is to be desorbed, more energy is required to remove an electron from the Fermi level in Al_2O_3 than from the Fermi level in MoS_2. This explains why coke is more strongly bonded to the alumina electron acceptor states.

The above discussion applies to the chemisorption of a single carbonaceous molecule. When a variety of species are being chemisorbed simultaneously, other changes such as the conversion of MoS_2 to MoS_3 can occur. This may result in changes in chemical bonding and changes in the position of the band edges. Nevertheless, the same general description should apply.

Evidence was presented earlier (72) for two kinds of coke on the catalyst surface. One is a reactive substance which is subsequently converted into reaction products. The other is an unreactive substance which blocks catalytic sites. The discussion presented here provides some basis for suggesting that the unreactive coke is chemisorbed predominantly on the alumina phase and that the reactive coke is chemisorbed predominantly on the molybdenum sulphide phase.

Promoter Effects

Several reviews have been published (34, 78-83) which have discussed the role of promoter as well as other aspects of Co-Mo-Al_2O_3 catalysts. The promoter has been described in terms of a separate phase intercalation model (84, 85), a synergy model involving hydrogen spillover (86), and a model in which both cobalt and molybdenum are present as a monolayer (87). The approach taken here follows that of Wentrcek and Wise (25-28), namely that the promoter improves the p-conductivity of the catalyst and therefore improves hydrogen-chemisorption. Their approach is compatible with some aspects of the other models described above.

In accordance with Equation 10, the promoter (usually cobalt or nickel) enhances the formation of electron holes. The action of the promoter is illustrated in Equation 18, where the sulphided promoter is analogous to that in Figure 4.

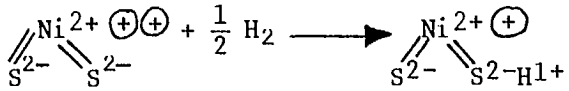

(18)

Data indicating the role of the promoter are shown in Figure 9. It is obvious that the nickel promoted catalysts cause much greater sulphur conversion than the catalysts containing molybdenum without nickel. The catalyst structure shown in Figure 4 indicates that the nickel (or cobalt) promoter should introduce electron holes and enhance p-conductivity (25, 28). Equations 10 and 18 indicate that electron holes enhance hydrogen chemisorption. Finally, Equation 14 indicates that a greater concentration of electron holes should cause a greater rate of conversion. Thus, the explanation presented here is consistent with the improvement in sulphur conversion caused by adding promoter to the catalyst, which is shown in Figure 9.

The nickel promoter has no effect on the amount of coke deposition on the catalyst, since catalysts with and without nickel fall on the same line in the lower part of Figure 9. The undesirable reactions (coke formation) should not be affected by electron holes, according to Equation 16. The data in Figure 9 show that adding the promoter did not produce any change in catalyst coke content. Therefore the data in Figure 9 support the explanation illustrated by Equation 16.

Additional evidence (55, 72) for the same phenomena are shown in Figure 11. These data also show that the beneficial promoters (cobalt and nickel) produce considerable enhancement of sulphur conversion with corresponding little effect on coke formation. Figure 11 supports the model given in Equations 14 and 16, if it is assumed that cobalt and nickel can enter into a solid solution with the molybdenum sulphide phase.

There have been some reports in the literature which suggest that the catalytic effect is caused by the promoter within the molybdenum sulphide phase. Wivel et al (88) reported a correlation between desulphurization rate constant and a Mossbauer signal which they related to the amount of promoter in the molybdenum sulphide phase. Earlier Richardson (89) reported a correlation

between the desulphurization rate constant and magnetic measurements which he related to the amount of promoter in the molybdenum sulphide phase. Candia et al (90) have characterized catalysts made by different methods and reported a relationship between the amount of cobalt in the Co-Mo-S phase and the catalytic activity. Topsoe et al (37) have recently suggested that the promoter is located either at the edges or within the bulk of the molybdenum sulphide phase. Farragher and Cossee (85) presented electron micrographs showing a progressive loss in crystallinity of molybdenum sulphide as the concentration of the promoter increased. These results could also support the suggestion of Topsoe et al (37) despite the fact that they were originally (85) explained in terms of intercalation.

Some effects of the promoter are also shown in Table 1. The conversions in Table 1 were obtained at 13.9 MPa and 400°C. It is seen that adding molybdenum to alumina produces a catalytic effect and that adding both molybdenum and a nickel promoter causes an even greater catalytic effect These phenomena have been reported frequently. Table 1 also shows that adding nickel to alumina also produces some catalytic effect, although it is less than that produced by adding molybdenum. Initially this part of Table 1 would appear to be contrary to other results reported in the literature. For example, Mitchell (91) states that both Al_2O_3 and $CoAl_2O_4$ are both inactive and that Co_9S_8 is insignificantly active. However, Mitchell's comments probably apply to reactions near atmospheric pressure, whereas the data in Table 1 were obtained at high pressure. DeBeer and Schuit (80, 92) have reported that a catalyst containing 4 percent MoO_3 was only slightly sulphided and was completely inactive in experiments performed near atmospheric pressure. In contrast, high pressure experiments (54) have shown catalysts of this composition to be extremely active. It was reported recently (93) that a 3% CoO-15% MoO_3-Al_2O_3 catalyst was only partially sulphided during atmospheric pressure experiments. In contrast at high pressures (94) the same catalyst was completely sulphided.

The catalytic effect caused by sulphided nickel on alumina can also be explained in terms of Equation 14. The alumina provides the electron acceptor states which chemisorb the hydrocarbon. The nickel sulphide may contain excess non-stoichiometric sulphur, thereby providing the electron holes which chemisorb hydrogen. For example, Krylov (31) has reported that nickel sulphide is a p-conductor (i.e. has electron holes).

Very recently hydrodesulphurization catalysts have been prepared using graphitized carbon supports (95-97). It has been suggested (96) that the promoter-carbon interaction would be weaker than the promoter-alumina interaction, and that a greater fraction of the promoter cations would be accessible to the reactants if a graphite-type catalyst support was used. For example, Galiasso (98) has reported that the promoter enters alumina during calcination and migrates to the surface again during sulphiding. In any event, sulphided promoter-graphite catalysts (without molybdenum) have produced high conversions. These results can also be explained in terms of Equation 14. The sulphided nickel (31) will provide the electron holes for hydrogen chemisorption. The resonating electron clouds (pi electrons) parallel to the basal planes of carbon atomns in the graphite can accept additional electrons. Therefore, these electron clouds are the electron acceptor states at which chemisorption of the carbonaceous molecules can occur.

Electron Donors and Acceptors

Studies have been reported in which alkali metal compounds (99) and halide compounds (100) have been added to catalysts. They act as electron donors and electron acceptors, respectively.

Changes caused by adding alkali metal compounds (99) to the catalyst are shown in Figure 12. Both the sulphur conversion and the amount of coke on the catalyst decreased with increasing amount of alkali metal compound. These effects can be explained in terms of the electronic and structural changes which they cause in the catalyst. For example, the addition of alkali metal compounds is known to decrease the catalyst surface area (99). Gamma Al_2O_3 has the spinel structure of $MgAl_2O_4$. The dimensions of Na^{1+} (97 pm) and K^{1+} (133 pm) are too large to occupy lattice positions of either Al^{3+} (51 pm) or Mg^{2+} (66 pm). Therefore, the alkali metal cations must occupy interstitial positions and cause at least a slight perturbation in the oxygen anion lattice of Al_2O_3.

The situation is similar in MoS_2. The dimensions of Mo^{4+} (70 pm) and Co^{2+} (72 pm) are smaller than those of the alkali metal cations. Also, the cation hole or vacancy between MoS_2 layers has been calculated by Farragher and Cossee (85) to be 74 pm. This is also too small to accommodate alkali metal cations. Therefore, any alkali metal cations would have to be present in interstitial positions. On this basis the orbitals of the alkali metal cations probably do not form energy bands of their own. Instead, the alkali metal cations probably donate electrons, for example, to the Al^{3+} conduction band of Al_2O_3.

Alkali metal cations will be present in the catalyst either as a discontinuity within the bulk, or on the surface of a colloidal particle within the catalyst. The equation at the top of Figure 13 illustrates sodium on the catalyst surface. Since sodium has a smaller electronegativity than aluminum, the electron density in the oxygen anion adjacent to the sodium cation will be higher than for oxygen anions in Al_2O_3 which does not contain sodium. The δ^- symbol indicates the larger electron density. Similarly the δ^+ symbol on the sodium indicates a smaller electron density than would be present on cations in sodium-free Al_2O_3. The effect of sodium's smaller electrongativity will be propagated from ion to ion. Thus, the δ^- symbol on the aluminum cation in Figure 13 also indicates a greater electron density than that on aluminum cations in sodium-free Al_2O_3. The net effect is that when sodium is present, the Al_2O_3 is slightly enriched in electrons. In other words sodium is effectively an electron donor.

The energy band diagram for the sodium containing catalyst is shown in the lower part of Figure 13. The greater electron density will cause the Fermi level in Al_2O_3 to increase, compared to that for intrinsic Al_2O_3, shown in Figure 10. The greater electron density in Al_2O_3 is illustrated by the electrons in the conduction band of the aluminum cations in Figure 13.

In principle at equilibrium the Fermi level should be the same in all solid phases. For present purposes the alumina may be considered as a bulk phase and the molybdenum sulphide as a surface phase. Since the energy band gaps are vastly different in Al_2O_3 and MoS_2, there will be some situations in which the Fermi levels in the two phases will be different. A surface space charge region (76, 101) will build up at the edge of at least one of the phases. In Figure 13, this would occur if electrons in the alumina phase were transferred to the MoS_2 phase. Band bending, shown in Figure 13, occurs in space charge regions. Although space charge regions can occur on both sides of a solid-solid interface, only one is show in Figure 13.

The data in Figure 12 can now be explained. The higher electron density in the alumina will inhibit the chemisorption of carbonaceous species conceptually by providing more electrons to the aluminum cation electron acceptor states. Electrons which have transferred to the sulphide phase can occupy the molybdenum cation electron acceptor states and also inhibit chemisorption of carbonaceous species. These effects should decrease sulphur conversion in accordance with Equation 14 and decrease catalyst coke content in accordance with Equation 16. Both of these trends are observed in Figure 12. If electrons are transferred from Al_2O_3 to MoS_2, they will annihilate electron holes. The elimination of some of the electron holes in MoS_2 should also decrease desirable reactions in accordance with Equation 14.

Halide ions should have substantially different effects than alkali metal ions. The addition of fluoride ions to the catalyst has been reported recently (100). At low concentrations fluoride ions are incorporated into the Al_2O_3 phase (102). At higher concentrations a separate AlF_3 phase is formed (102). The beta modification of AlF_3 has been reported (103, 104) to form smaller crystals which provide greater surface areas and greater reactivities. The present discussion is restricted to the presence of fluoride ions in low concentrations.

The equation at the top of Figure 14 represents fluorine on a catalyst surface. It is consistent with the work of Scokart et al (102) who have reported that fluoride ions replace hydroxyl groups at the catalyst surface. Fluorine has a large electronegativity. Electrons will be strongly attracted toward it. Therefore the electron density at its neighboring aluminum cation will be lower than at an aluminum cation in fluorine-free alumina. This effect will also be propogated from ion to ion. As before δ^- and δ^+ represent an enhancement and a deficiency of electrons respectively. The net effect is that when fluorine is present, the Al_2O_3 will have a slight deficiency in electrons (or enrichment in electron holes), compared to fluorine-free alumina. In other words, fluorine is essentially an electron acceptor.

The energy band diagram for the fluorine containing catalyst is shown in the lower part of Figure 14. The lower electron density in the Al_2O_3 phase will cause the Fermi level to decrease. The position of the Fermi level will be controlled by the concentration of fluorine anions in the Al_2O_3 phase. The lower electron density in Al_2O_3 is illustrated by the electron holes in the valence band of oxygen anions in Figure 14.

These concepts can be used to explain the data which has been reported for catalysts containing fluorine (100). The lower electron density should increase the strength of the chemisorption band between the aluminum cation electron acceptor states and the carbonaceous species. In other words, the aluminum electron acceptor states should attract carbonaceous species more readily. This may increase the catalyst coke content. The transference of electron holes to the MoS_2 surface phase should also increase the number of catalyst sites for desirable reactions, in accordance with Equation 14. The data (100, 105) clearly show that the presence of fluorine in the catalyst enhances desirable reactions.

GASIFICATION

During gasification, higher molecular weight materials such as coal, char, or residuum are converted to hydrogen and a molecule containing one carbon atom. The type of gasification considered here is the reaction of steam with a carbonaceous material, to produce carbon monoxide and hydrogen. A single step process to gasify coal and convert the CO and H_2 to methane using a potassium carbonate catalyst is being developed (106). It has been demonstrated at the one ton per day scale (107). A dual reactor system using an alkaline earth metal-transition metal catalyst has also been tested at the pilot-scale (108).

The role of the catalyst in the gasification reaction is of primary interest in this discussion. Earlier studies by Long and Sykes (109) and by Croft (110) have suggested that there is a transfer of electrons between the catalyst and the carbonaceous solid. More recently, McKee and Chatterji (111) and also Veraa and Bell (112) have explained the function of the catalyst in terms of a series of reactions involving the reduction of potassium carbonate and its subsequent regeneration. However, some of the catalytic species which they postulated were not detected in recent x-ray photoelectron spectroscopy-measurements (113). Wen (114) reviewed the mechanisms of alkali metal catalysis during gasification. He has described the electronic band structure of graphite in terms of a two dimensional model, [Roberts et al (115) and Herpin (116)], which was based on the earlier work of McDonnell et al (117). His model suggests that n-type catalysts would donate electrons to the graphite and that p-type catalysts would accept electrons from graphite.

Experiments in which there was a step change in temperature and also other experiments in which there was a step change in the steam concentration have indicated (118) that hydrogen is produced very quickly. In contrast, carbon monoxide is produced very slowly. This suggests that the steam reacts with the carbon to produce hydrogen virtually instantaneously, and the remaining hydroxyl groups react more slowly. They are probably chemisorbed more strongly to the carbonaceous material. By examining partially reacted chars at liquid nitrogen temperature, using X-ray photoelectron spectroscopy, different types of oxygen bonding to carbon have been observed. Liquid nitrogen temperatures were necessary in order to prevent the reaction species on the catalyst from being pumped off under the high vacuum conditions present in the spectrometer. The results suggest an enol-keto transformation in which hydroxyl oxygen becomes carbonyl oxygen.

Steam gasification of (A), char without additives, has been compared with (B), char containing a potassium salt catalyst, and with (C), char containing a vanadium oxide inhibitor (113). An Arrhenius plot indicated that the activation energy decreased slightly with the potassium catalyst and increased slightly with the vanadium inhibitor. Nevertheless, all three activation energies were very similar, and the lines on the Arrhenius plot were more or less parallel. However, they all had different intercepts. Since this Arrhenius plot was made in terms of log rate vs $\frac{1}{T}$, the ordinate is probably indicative of the number of catalyst sites. This suggests that the presence of the catalyst increases the number of reaction sites and the presence of the inhibitor probably decreases the number of reaction sites. An older study by Taylor and Neville (119) showed that the carbon-steam reaction increased linearly with the amount of K_2CO_3 catalyst added to the char, up to 20 weight percent. This also suggests that the catalyst may be introducing additional catalytic sites. As described above, the slow step in the reaction has been shown to be the evolution of carbon monoxide (118). To form carbon monoxide, a triple bond between a surface oxygen atom and a carbon atom must be formed. The transition state might involve a carbon atom at an edge plane in the carbonaceous solid. The precursors will probably be double bonds between surface oxygen and edge plane carbon atoms. Presumably carbon pi electrons and electrons donated by the catalyst will be borrowed to form the triple bond, in the transition state. When the sigma bonds between the reacting carbon atom (in the CO to be formed) and its neighboring carbon atoms have been broken, the proper number of electrons will again be associated with the pi clouds and the catalyst.

When vanadium is present, some of the pi electrons associated with carbon layers may enter its vacant d-orbitals. This will decrease the number of pi electrons available at the carbon edge plane reaction sites. Thus, vanadium- should be an inhibitor. In contrast, potassium can donate its outer electron to the pi electron clouds. Therefore, potassium should be a catalyst.

These results can also be explained qualitatively in terms of the energy band diagram shown in Figure 15. These diagrams were constructed by combining the information reported by McDonnell et al (117) and by Bach et al (120). They are slightly different than those suggested by Wen (114). They show that the potassium catalyst donates electrons to the carbon bands and raises the Fermi level while the vanadium inhibitor withdraws electrons and decreases the Fermi level. It is inferred that the addition (or withdrawl) of electrons by the catalyst (or inhibitor) increases (or decreases) the number of catalytic sites. On this basis an electronic mechanism can explain catalysis of steam-char gasification.

NATURAL GAS CONVERSION

The conversion of natural gas to liquid fuels may be highly desirable if and when the economics of such conversion technology are favorable. For example, Canada imports large quantities of crude oil. At the present time there are ample proven reserves of natural gas. Conversion of natural gas to liquid hydrocarbons would decrease crude oil imports and have a desirable effect on the country's balance of payments.

In New Zealand, the construction of a facility to convert natural gas to gasoline has been announced (121). Natural gas will first be steam reformed to produce a mixture of carbon monoxide and hydrogen. The second process will convert this mixture to methanol. Commercially proven processes will be used for both of these steps. The third step will be the conversion of methanol to gasoline in a fixed bed reactor using the new methanol to gasoline (MTG) process which has been developed in recent years (122). This will be the first commercial scale plant using the MTG process.

An alternative technology has been proposed by Benson (123). He has suggested a single process. In principle a single step process could have a much lower capital cost than the sequence of three processes to be used in New Zealand. In Benson's process natural gas and chlorine react to form higher molecular weight hydrocarbons. The principle products are ethane, ethylene, hydrogen chloride and hydrogen. Subsequently the hydrogen chloride can be burned with air to form water and chlorine. The chlorine can be recycled to react with additional methane. In principle it should be possible to polymerize ethylene to produce fuels of desirable quality.

The thermodynamic driving force is one of the factors to be considered in developing natural gas conversion processes. The free energies of formation of compounds composed of carbon and hydrogen are shown in Figure 16. It will be thermodynamically favorable for methane to be converted to any product which has a lower free energy. Figure 16 indicates that carbon, acetylene, and ethylene are potential products at higher temperatures. Fang and Yeh (124) have recently reported that acetylene and ethylene are among the reaction products from methane conversion.

As the reaction products (acetylene and ethylene) are cooled to ambient temperature, the possibility of forming higher molecular weight hydrocarbons exists. This can be seen from the curves in Figure 17. For example, at lower temperatures, the free energy of formation of acetylene is higher than that of hexane (paraffins) and of benzene (aromatics). Therefore, at lower temperatures there will be a thermodynamic driving force for the formation of paraffins and of aromatics from acetylene. On the basis of this discussion a single step process for methane conversion could consist of a higher temperature reactor, followed by a lower temperature reactor. Methane would be converted to acetylene and ethylene in the higher temperature reactor. These products would be converted to paraffins and/or aromatics in the lower temperature reactor.

Catalysts having high selectivity for the desired products could be used. For the lower temperature reactor a catalyst which selectively produced aromatics would be necessary if gasoline was the desired product. Alternatively, if diesel fuel was the desired product, the catalyst should selectively produce paraffins. For the higher temperature reactor a catalyst which has a very low selectivity for carbon formation will be essential.

A catalytic mechanism for methane conversion in solution was proposed by Olah et al (125). They concluded that superacids (stronger than sulphuric acid) were responsible for catalyzing the reaction. Of course, at the temperatures used in their work, the yields of products were extremely small. Lefebvre and Sajus (126) extended this concept to the use of solid superacid catalysts. Tanabe (127) has recently reviewed the characteristics of solid acid catalysts.

In an earlier part of this paper it was noted that Lewis acid sites on solid catalysts can be described as electron acceptor states. In some cases Bronsted acid sites can be described as electron holes. Thus, electronic concepts may also prove to be useful in the development of catalysts for methane conversion.

CONCLUSIONS

The role of catalysts in changing the molecular weight of carbonaceous molecules in fossil fuels has been described. Electronic concepts have been used to explain experimental data obtained with hydrocracking catalysts and with gasification catalysts. Electronic concepts may also be useful in developing catalysts for methane conversion. It may be unequivocally stated that the electronic concepts which have been used here to explain hydrocracking catalysis provide a qualitative explanation for most data produced in our laboratory during the past ten years. However, a substantial amount of additional work will be required to produce a quantitative explanation.

REFERENCES

(1) Andrews, G.F., Lewis, H.M. and Dobson, E.S., Preprints, Am. Chem. Soc. Div. Petrol. Chem. 13 (2), F5 (1968).

(2) Gray, G.R., AIChE Symp. Ser. No. 127, 69, 99 (1973).

(3) Galbreath, R.B. and Van Driesen, R.P., Proc. 8th World Petrol. Congr. 4, 135 (1971).

(4) Menzies, M.M., Silva, A.E. and Denis, J.M., Chemical Engineering, Feb. 23, 1981, p. 46.

(5) Lunin, G., Silva, A.E. and Denis, J.M., Chemistry in Canada, March, 1981, p. 17.

(6) Bartsch, R. and Tanielian, C., J. Catal. 35, 353 (1974), J. Catal. 50, 35 (1977).

(7) Sternberg, H.W., Donne, C.L.D., Markby, R.E. and Friedman, S., Ind. Eng. Chem. Proc. Des. Dev. 13, 435 (1974).

(8) Nagai, M., Urimoto, H. and Sakikawa, N., Nippon Kagaku Kaishi (No. 2), 356 (1975).

(9) Houalla, M., Broderick, D., de Boer, V.H.J., Gates, B.C. and Kwart, H., Preprints, Am Chem Soc., Div Petrol Chem 22 (3), 941 (1977).

(10) Klemm, L.H. and Karchesy, J.J., J. Heterocycl Chem 15, 65 (1978).

(11) Dhainaut, E., Gachet, C. and deMourgues, L., C.R. Hebd. Seances, Acad. Sci. Series C; 288, 338 (1979).

(12) Geneste, P., Amblard, P., Bonnet, M. and Graffin, P., J. Catal 61, 115 (1980).

(13) Rollmann, L.D., J. Catal. 46, 243 (1977).

(14) Shih, S., Reiff, E., Zawadzki, R. and Katzer, J.R., Preprints, Am Chem Soc, Div Fuel Chem 23(1), 99 (1979).

(15) Katzer, J.R. and Sivasurbramanian, R., Catal Rev Sci Eng 20(2), 155 (1979).

(16) Cocchetto, J.F. and Satterfield, C.N., Ind Eng Chem Proc Des Dev 15, 272 (1976).

(17) Shabtai, J., Veluswamy, L. and Oblad, A.G., Preprints, Am Chem Soc, Div Fuel Chem 23(1), 114 (1980).

(18) Hung, C.W. and Wei, J.; Ind Eng Chem Proc Des Dev 19, 250; ibid p 257 (1980).

(19) Cowley, S.W. and Wiser, W.H.; Fuel Proc Technol 2, 317 (1979).

(20) Shabtai, J., Veluswamy, L. and Oblad, A.G., Am Chem Soc, Div. Fuel Chem, 23(1), 107 (1978).

(21) Dekker, J., Nell, B.C.K. and Potgieter, H.G.J., Fuel 57, 361 (1978).

(22) Sapre, A.V. and Gates, B.C., Ind Eng Chem Proc Des Dev 20, 68 (1981).

(23) Nakatsuji, Y., Kubo, T., Nomura, M. and Kikkawa, S., Bull Chem Soc, Japan 51, 618 (1978).

(24) Aoshima, A. and Wise, H., J. Catal 34, 145 (1975).

(25) Wentrcek, P.R., and Wise, H., J. Catal. 45, 349 (1976).

(26) Wentrcek, P.R., and Wise, H., Preprints, Am Chem Soc, Div Petrol Chem 22(2), 525 (1977).

(27) Wise, H., Proc. 2nd Intern. Conf. Chemistry and Uses of Molybdenum, (eds. p.c.h. Mitchell and A. Seaman), Climax Molybdenum, London (1977), p. 160.

(28) Wentrcek, P.R. and Wise, H., J. Catal. 51, 80 (1978).

(29) Wright, C.J., Sampson, C., Fraser, D., Moyes, R.B., Wells, P.B. and Riekel, C., J. Chem. Soc. Faraday I, 76, 1585 (1980).

(30) Ternan, M., "Electronic Concepts Applied to Coke Formation on Hydrocracking and Hydrodesulphurization Catalysts", Preprints, 6th Can. Symp. on Catal. 6, 220 (1979).

(31) Krylov, O.V., Catalysis by Non-metals, Academic Press New York, 1970, p.254.

(32) Williams, R.H. and McEvoy, A.J., Phys. Status Solidi 47, 217 (1971).

(33) McGovern, J.T., Williams, R.H., and Mee, C.H.B., Surf. Sci. 46, 427 (1974).

(34) Schuit, G.C.A., Int. J. Quant. Chem. 12 (S2) 43, 1977.

(35) Huisman, R., DeJonge, R., Haas, C. and Jellinek, F., J. Solid State Chem 3, 56 (1971).

(36) Hass, C., "Crystal Structure and Chemical Bonding in Inorganic Chemistry", (eds C.Y.M. Rooymans and A. Rabenau), North Holland, Amsterdam, 1975.

(37) Topsoe, H., Clausen, B.S., Candia, R., Wivel, C., and Morup, S., Bull. Soc. Chim. Belg. 90, 1208 (1981).

(38) Topsoe, H., Clausen, B.S., Candia, R., Wivel, C., and Morup, S., J. Catalysis 68, 449 (1981).

(39) Morrison, S.R., Surf. Sci. 50, 329 (1975).

(40) Shibata, K., Kiyoura, T., Kitagawa, J., Sumiyoshi, T., and Tanabe, K., Bull Chem Soc Japan 46, 2985 (1973).

(41) Tanabe, K., Sumiyoshi, T., Shibata, K., Kryoura, T., and Kitagawa, J., Bull Chem Soc Japan 47, 1064 (1974).

(42) Heckelsberg, L.F. and Banks, R.L., Preprints, Am Chem Sor, Div Petrol Chem 22(1), 19 (1977).

(43) Kittel, C., Introduction to Solid State Physics, 3rd ed., Wiley, New York, 1967, p. 474.

(44) Lippens, B.C. and Steggerda, J.J., in Physical and Chemical Aspects of Adsorbents and Catalysts (ed. B.G. Liasen), Academic Press, New York, 1970, pp 190-192.

(45) Tanabe, K. and Nishizaki, T., Proc. 6th Intern. Congr. Catal. v. 2, (eds. G.C. Bond, P.B. Wells and F.C. Tompkins), Chem. Soc., London, 1977, p. 863.

(46) Lipsch, J.M.J.G. and Schuit, G.C.A., J. Catal. 15, 179 (1969).

(47) Schuit, G.C.A. and Gates, B.C., AIChE J. 19, 417 (1973).

(48) Voorhoeve, R.J.H. and Stuiver, J.C.M., J. Catal. 23, 228 (1971).

(49) Perry, R.H. and Chilton, C.H., Chemical Engineers Handbook, 5th ed., McGraw-Hill, New York, 1973. pp 3-119, 3-147.

(50) Hougen, O.A., Watson, K.M. and Ragatz, R.A., "Chemical Process Principles, Wiley, New York, vol. 1 and 2 (1959).

(51) Desikan, P. and Amberg, C.H., Can. J. Chem. 42, 843 (1954).

(52) Tanaka, K., Okuhara, T., Sato, S., and Miyahara, K., J. Catal 43, 360 (1976).

(53) Massoth, F.E., J. Catal. 47, 316 (1977).

(54) Parsons, B.I. and Ternan, M., Proc. 6th Intern. Congr. Catal. (eds. G.C. Bond, P.B. Wells and F.C. Tompkins), Chem. Soc., London, 1977, p. 965.

(55) Ternan, M., ibid pp 945-6.

(56) Perry, R.H. and Chilton, C.H., Chemical Engineers' Handbook, 5th ed., McGraw-Hill, New York, 1973, p. 3-91.

(57) Pauling, L., "The Nature of the Chemical Bond", 3rd ed., Cornell University Press, Ithaca, 1960, p. 262.

(58) DeBeer, V.H.J., Bevelander, C., Van Sint Fiet, T.H.M., Werter, P.G.A., and Amberg, C.H., J. Catal 43, 68 (1976).

(59) Broderick, D.H., Schuit, G.C.A. and Gates, B.C., Preprints, Div. Fuel Chem, Am. Chem. Soc. 23(1), 92 (1978).

(60) Owens, P.J. and Amberg, C.H., Advan. Chem. 33, 186 (1961).

(61) Hagenbach, G., Courty, Ph., and Delmon, B., J. Catalysis 31, 264 (1973).

(62) Vrinat, M.L., Gachet, C.G., Cavalletto, G., and DeMourgues, App. Catal. 3, 57 (1982).

(63) Metcalfe, T.B., Chim. Ind. Gen. Chim. 102, 1300 (1969).

(64) Ternan, M. and Whalley, M.J., Can. J. Chem. Eng. 54, 642 (1976).

(65) Massoth, F.E., Chung, K.S., and Ramachandran, R., Fuel Proc. Techol 2, 57 (1979).

(66) Brewer, M.B. and Cheavens, T.H., Hydrocarbon Proc. 45 (4), 203, April (1966).

(67) DeBeer, V.H.J., Ph.D. Thesis, Eindhoven University of Technology, p. 60 (1975).

(68) Morup, S., Clausen, B.S., and Topsoe, H., J. Phys. (France) Colloque 40, C2-88 (1979).

(69) Brown, J.R. and Ternan, M., Preprints, Can. Symp. Catal. 8, 4 (1982).

(70) Ternan, M., Packwood, P.H., Buchanan, R.M., and Parsons, B.I., Can. J. Chem. Eng. 60, 33 (1982).

(71) Bancroft, G.M., Gupta, R.P., Hardin, A.H., and Ternan, M., Anal. Chem. 51, 2101 (1979).

(72) Ternan, M., Furimsky, E. and Parsons, B.I., Fuel Proc. Technol. 2, 45 (1979).

(73) Wolkenstein, Th., Adv. Catal. 12, 189 (1960).

(74) Basolo, F. and Johnson, R., "Coordination Chemistry", Benjamin, New York (1964).

(75) Hayward, D.O. and Trapnell, B.M.W., "Chemisorption", 2nd ed., Butterworths, London (1964).

(76) Many, A., Goldstein, Y. and Grover, N.B., Semiconductor Surfaces, North Holland, Amsterdam (1971).

(77) Sebera, D.K., "Electonic Structure and Chemical Bonding", Blaisdell (Ginn), Walthan, Massachusetts, 1964.

(78) Amberg, C.H., J. Less Common Metals, 36, 339 (1974).

(79) Grange, P., Catal. Rev. Sci. Eng. 21, 135 (1980).

(80) deBeer, V.H.J., and Schuit, G.C.A., Ann. N.Y. Acad. Sci. 272, 61 (1976).

(81) Massoth, F.E., Adv. Catal. 27, 265 (1978).

(82) Delmon, B., Int. Chem. Eng. 20 (4), 639 (1980).

(83) Ratnasamy, P. and Sivasanker, S., Catal. Rev. Sci. Eng. 22, 401 (1980).

(84) Voorhoeve, R.J.H. and Stuiver, J.C.M., J. Catal. 23, 243 (1971).

(85) Farragher, A.L. and Cossee, P., Proc. 5th Intern. Congr. Catalysis (North Holland, Amsterdam, 1973) p. 1301.

(86) Delmon, B., React. Kinet. Catal. Lett 13, 203 (1980).

(87) Massoth, F.E., J. Catal 50, 195 (1977).

(88) Wivel, C., Candia, R., Clausen, B.S., Morup, S., and Topsoe, H., J. Catal 68, 453 (1981).

(89) Richardson, J.T., Ind. Eng. Chem. Fund. 3, 151 (1964).

(90) Candia, R., Clausen, B.S., and Topsoe, H., Bull. Soc. Chim. Belg. 90, 1225 (1981).

(91) Mitchell, P.C.H., "The Chemistry of Some Hydrodesulphurization Catalysts Containing Molybdenum", Climax Molybdenum Co. Ltd., London, 1967.

(92) DeBeer, V.H.J., Van der Aalst, M.J.M., Machiels, C.J., and Schuit, G.C.A., J. Catal. 43, 78 (1976).

(93) Brown, J.R. and Ternan, M., Preprints, Am. Chem. Soc., Div. Petrol. Chem. 27, 742 (1982).

(94) Brown, J.R. and Logie, R.B., unpublished results.

(95) Breysse, M., Bennett, B.A., and Chadwick, D., J. Catal. 71, 403 (1981).

(96) DeBeer, V.H.J., Duchet, J.C., and Prins, R., J. Catal. 72, 369 (1982).

(97) Stevens, G.C., and Edmonds, T., in "Preparation of Catalysts II", (B. Delmon, Ed.), p. 507 Elsevier, Amsterdam, 1979.

(98) Galiasso, R., Preprints, Am. Chem. Soc., Div. Petrol. Chem. 27, 981 (1982).

(99) Kelly, J.F. and Ternan, M., Can. J. Chem. Eng. 57, 726 (1979).

(100) Boorman, P.M., Kriz, J.F., Brown, J.R. and Ternan, M., "Co-Mo-Al_2O_3 Catalysts in the Hydrocracking of Athabasca Bitumen: Effects of the Presence of Na and F on Their Composition and Performance." IV International Conference on the Chemistry and Uses of Molybdenum, Colorado, August 1982, p. 35.

(101) Clark, A., "The Chemisorptive Bond", p. 82, Academic Press, New York, 1974.

(102) Scokart, P.O., Selim, S.A., Damon, J.P., and Rouxhet, P.G., J. Colloid Inter. Sci. 70, 209 (1979).

(103) Kowalak, S., Acta Chimica Sci. Hung. 107, 19 (1981).

(104) Kowalak, S., ibid, p. 27.

(105) Boorman, P.M., Kriz, J.F., Brown, J.R., and Ternan, M., unpublished results.

(106) Kalina, T. and Nahas, N.C., "Exxon Coal Gasification Process Predevelopment Program", National Technical Information Service Report FE-2369-24, U.S. Department of Commerce, Springfield, Virginia (1978).

(107) Kaplan, L.J., Chemical Engineering 89 (6), 64 (1982).

(108) Furaki, M. and Ueda, M., J. Inst. Fuel, 38 (1978).

(109) Long, F.J. and Sykes, K.W., Proc. Roy. Soc. A215, 100 (1952).

(110) Croft, R.C., Austr. J. Chem. 9, 194 (1956).

(111) McKee, D.W. and Chatterji, D., Carbon 16, 53 (1978).

(112) Veraa, M.J. and Bell, A.T., Fuel 57, 194 (1978).

(113) Sekhar, M.V.C. and Ternan, M., Fuel Proc. Techn. 6, 61 (1982).

(114) Wen, W.Y., Catal. Rev. Sci. Eng. 22, 1 (1980).

(115) Roberts, M.C., Oberli, M., and Mering, J., Chem. Phys. Carbon 10, 141 (1978).

(116) Herpin, A., in Les Carbones, Vol. 1, Masson, Paris, 1965, p. 211.

(117) McDonnell, F.R., Pink, R.C. and Ubbelohde, J. Chem. Soc. 191 (1951).

(118) Ternan, M., Sekhar, M.V.C. and Packwood, R.H., "The Catalytic Steam Gasification of Chars by K_2CO_3, "Divisional Report ERP/ERL 81-45(J). Department of Energy, Mines and Resources, Ottawa, 1981.

(119) Taylor, H.S. and Neville, H.A., J. Am. Chem. Soc. 43, 2055 (1921).

(120) Bach, B., Evans, E.L., Thomas, J.M., and Barber, M., Chem. Phys. Lett. 10, 547 (1971).

(121) Anon, Chem. Eng., Oct. 5, 1981, p. 36.

(122) Morgan, C.R., Warner, J.P., and Yurchak, S., Ind. Eng. Chem. Prod. Res. Dev. 20, 185 (1981).

(123) Benson, S.W., "Conversion of Methane", U.S. Patent 4,199,533, April 22, 1980.

(124) Fang, T. and Yeh, C.T., J. Catal 69, 227 (1981).

(125) Olah, G.A., Klopman, G. and Schlosberg, R.H., J. Am. Chem. Soc. 91, 3261 (1969).

(126) Lefebvre, G. and Sajus, L., 8th World Petrol. Congr. 4, 283 (1971).

(127) Tanabe, K., "Catalysis-Science and Technology", (eds., J.R. Anderson and M. Boudart), Springer-Verlag, Berlin, p. 232 (1981).

TABLE 1

SULPHUR CONVERSIONS WHEN HYDROTREATING A 345-525°C
GAS OIL WHICH WAS DERIVED FROM ATHABASCA BITUMEN

Oxide Form of Catalyst	Sulphur Conversion m %
100% Al_2O_3	1.4
2.2% MoO_3 - Balance Al_2O_3	33.2
1.14% NiO, 2.2% MoO_3 - Balance Al_2O_3	74.9
1.14% NiO - Balance Al_2O_3	23.8

LIST OF FIGURES

Figure 10. Energy Band Diagram Comparing Relative Band Gaps and Fermi Levels in Intrinsic Al_2O_3 and Intrinsic MoS_2.

Figure 11. Conversion of Sulphur Containing Carbonaceous Species at 400°C (mass per cent) and Statistical Number of Coke Layers on the Catalyst versus Promoter Cation in sulphided Mo-Al_2O_3 Catalysts. The metal cation to molybdenum atomic ratio was 1.0. Circles and squares represent catalysts calcined at 500°C and 900°C respectively. Data from refernce (54).

Figure 12. Conversion of Sulphur Containing Carbonaceous Species and Statistical Number of Coke Layers Versus the Alkali Metal to Molybdenum Atomic Ratio. All catalysts contained 2.2 m % MoO_3 and 1.1 m % CoO in their oxide form. DAta from reference (99).

Figure 13. Sodium in Sulphided Mo-Al_2O_3 Catalysts. Top: Location of Sodium on the Catalyst Surface. Bottom: Effects of Sodium on the Energy Band Diagrams.

Figure 14. Fluorine in Sulphided Mo-Al_2O_3 Catalysts. Top: Location of Fluorine on the Catalyst Surface. Bottom: Effects of Fluorine on the Energy Band Diagrams.

Figure 15. Electron Energy E, for the C2s band versus density of states N(E), for graphite plus potassium, graphite only, and graphite plus vanadium.

Figure 16. Free Energy of Formation Function ($\Delta G/RT$) Versus Temperature (K) for C1 and C2 Hydrocarbons.

Figure 17. Free Energy of Formation Function ($\Delta G/RT$) Versus Temperature (K) for Aromatics (C_6H_6) and Paraffins (C_6H_{14}) compared to Ethylene and Acetylene.

HYDRODESULPHURIZATION + HYDRODEOXYGENATION

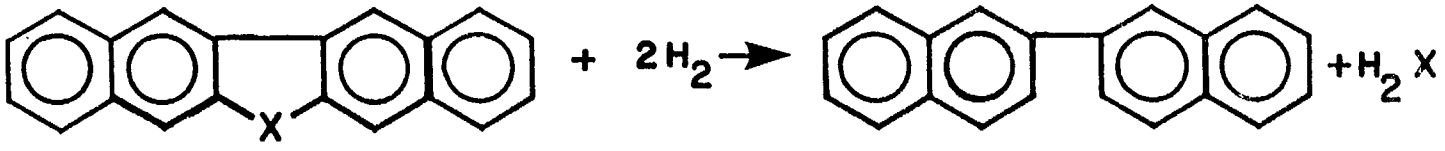

X = S or O

X = S or O

HYDRODENITROGENATION

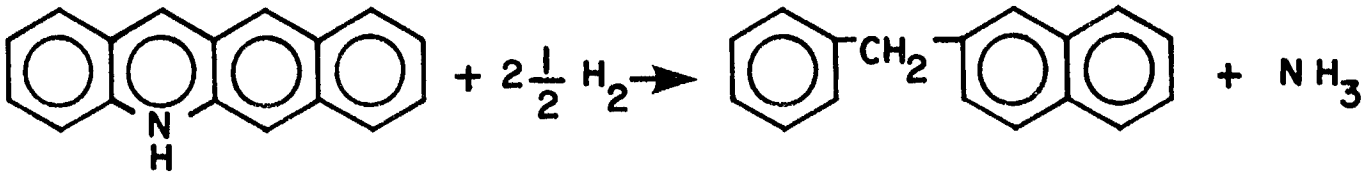

HYDRODEMETALLIZATION

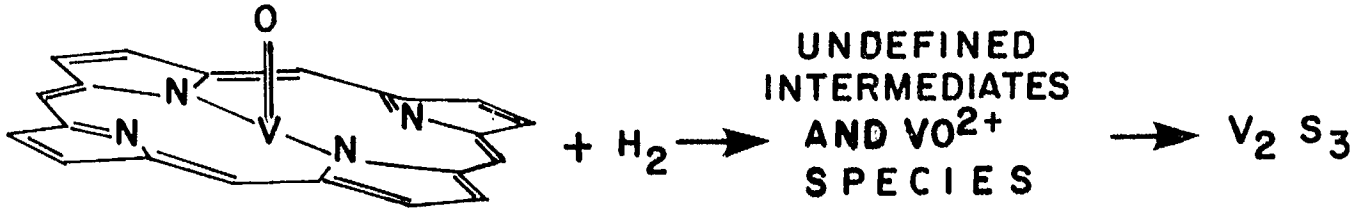

MOLECULAR WEIGHT REDUCTION

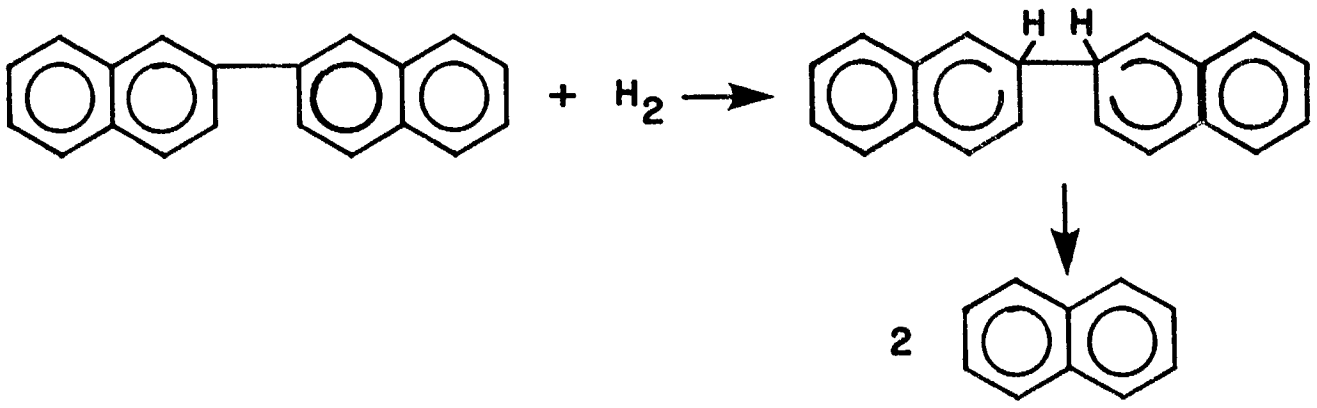

Fig 1

MoS_2

A

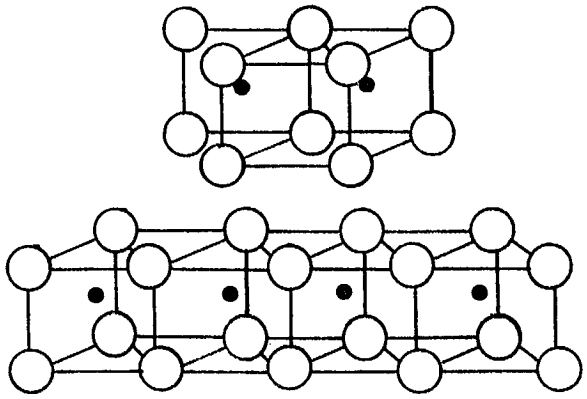

B

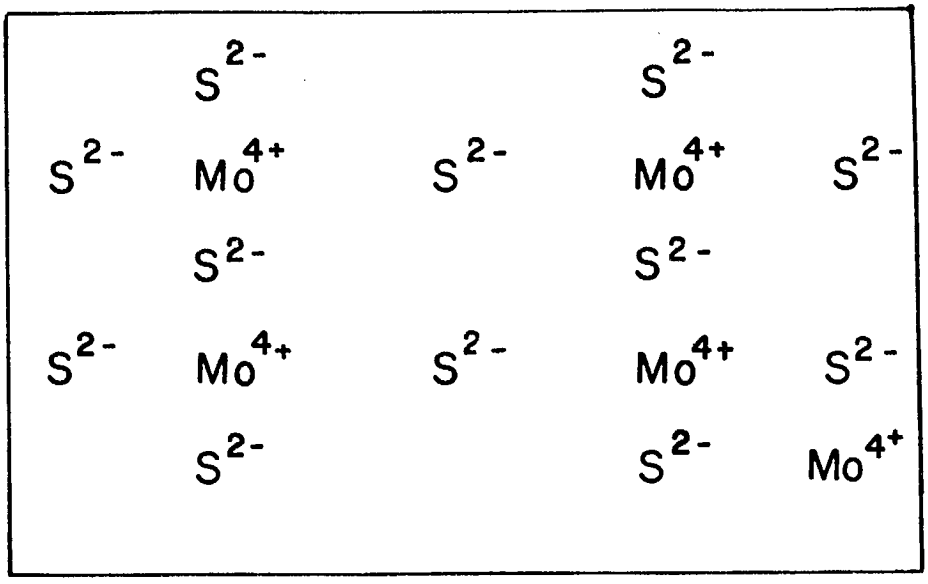

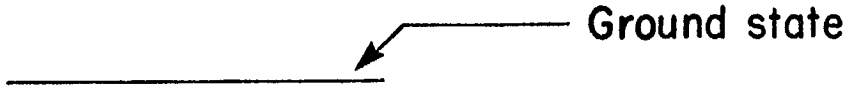

C

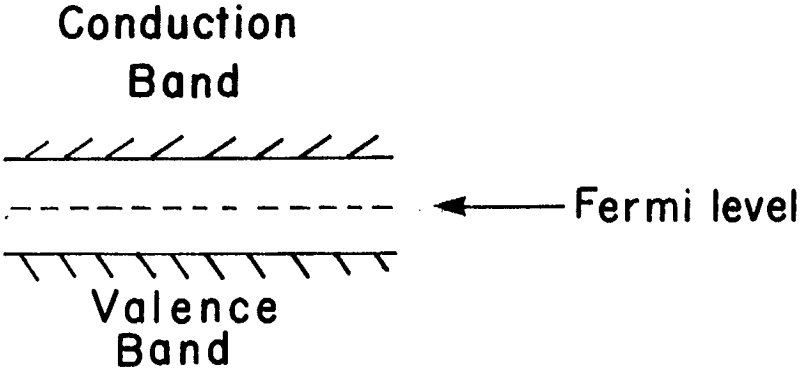

FIG 2

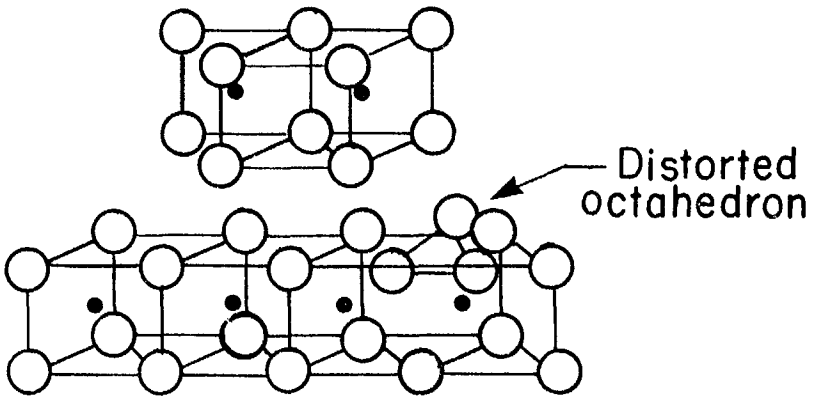
Distorted
octahedron

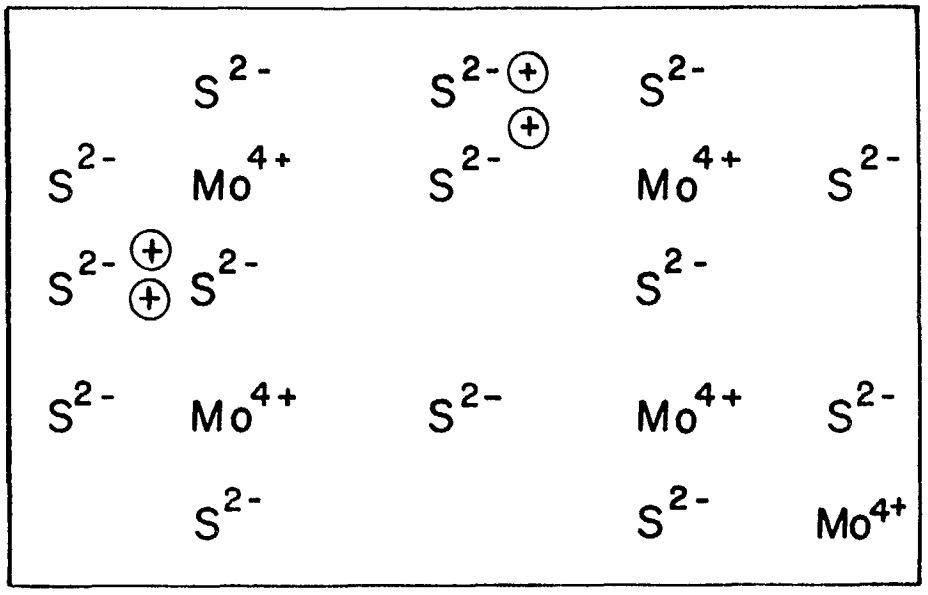
S2-
S2-
S2-
S2-
Mo4+
S2-
Mo4+
S2-
S2-
S2-
S2-
S2-
Mo4+
S2-
Mo4+
S2-
S2-
S2-
Mo4+

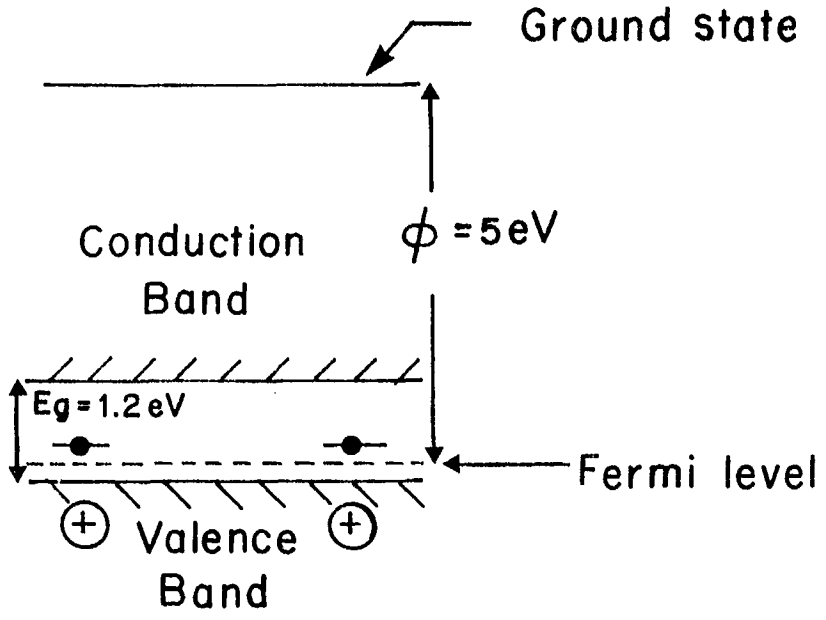
Ground state
Conduction
Band
ϕ =5eV
Eg=1.2eV
Fermi level
Valence
Band

FIG 3

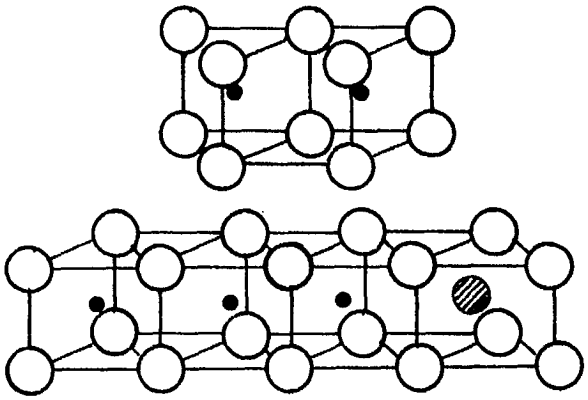

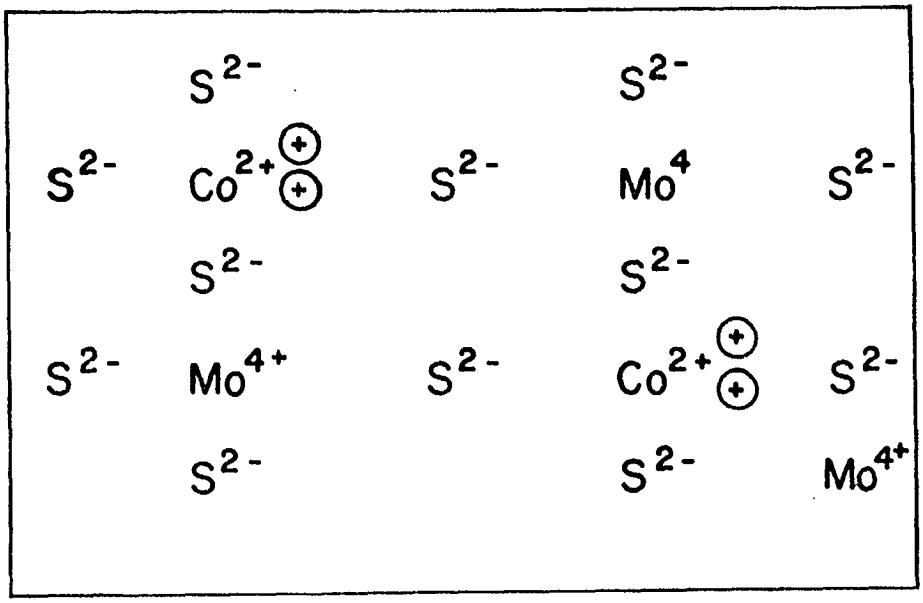
S2-
S2-
S2-
Co2+
S2-
Mo4
S2-
S2-
S2-
S2-
S2-
Mo4+
S2-
Co2+
S2-
S2-
S2-
Mo4+

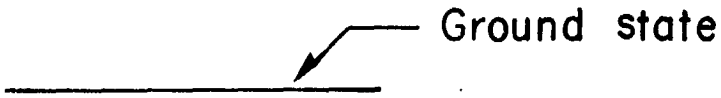
Ground state

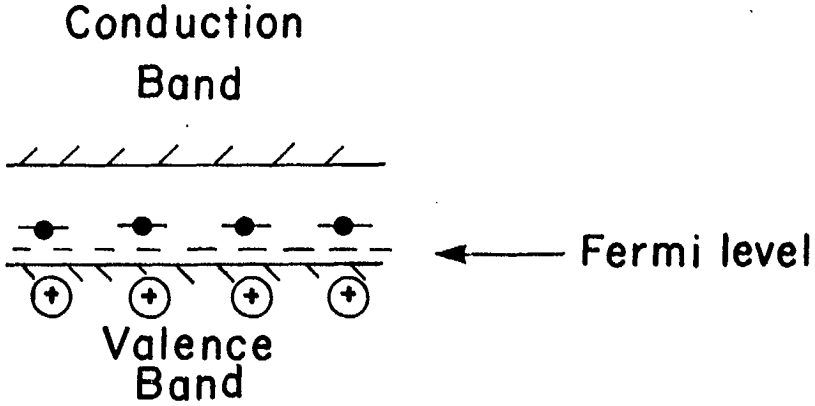
Conduction
Band
Fermi level
Valence
Band

FIG 4

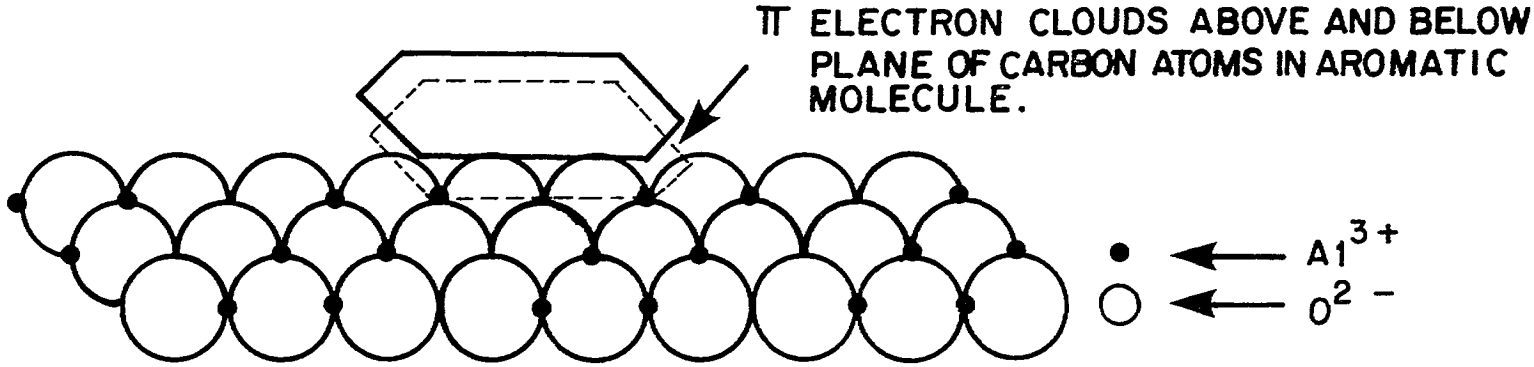
π ELECTRON CLOUDS ABOVE AND BELOW PLANE OF CARBON ATOMS IN AROMATIC MOLECULE.
Al^{3+}
O^{2-}

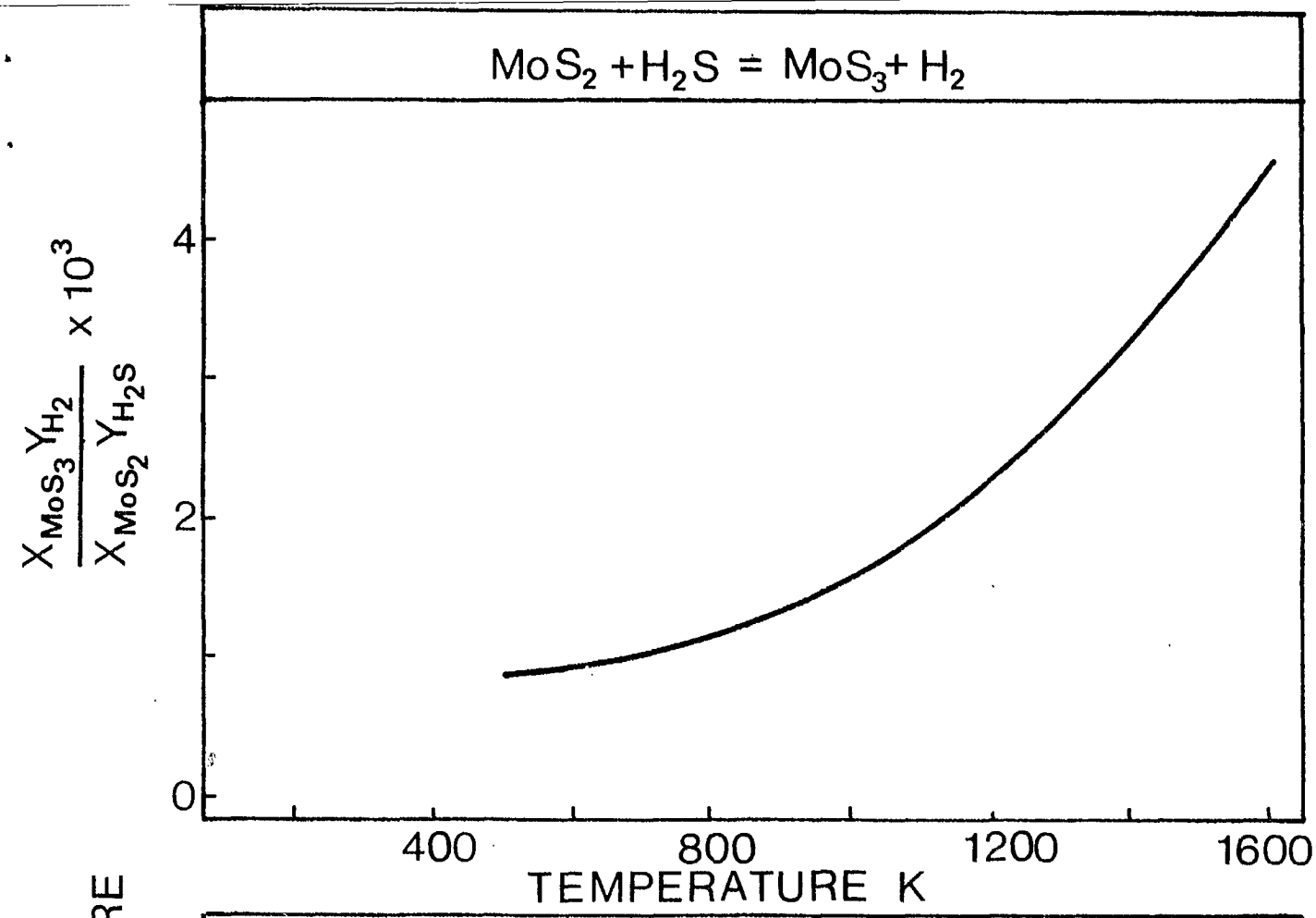
$MoS_2 + H_2S = MoS_3 + H_2$
$\frac{X_{MoS_3} Y_{H_2}}{X_{MoS_2} Y_{H_2S}} \times 10^3$
0
2
4
400
800
1200
1600
TEMPERATURE K

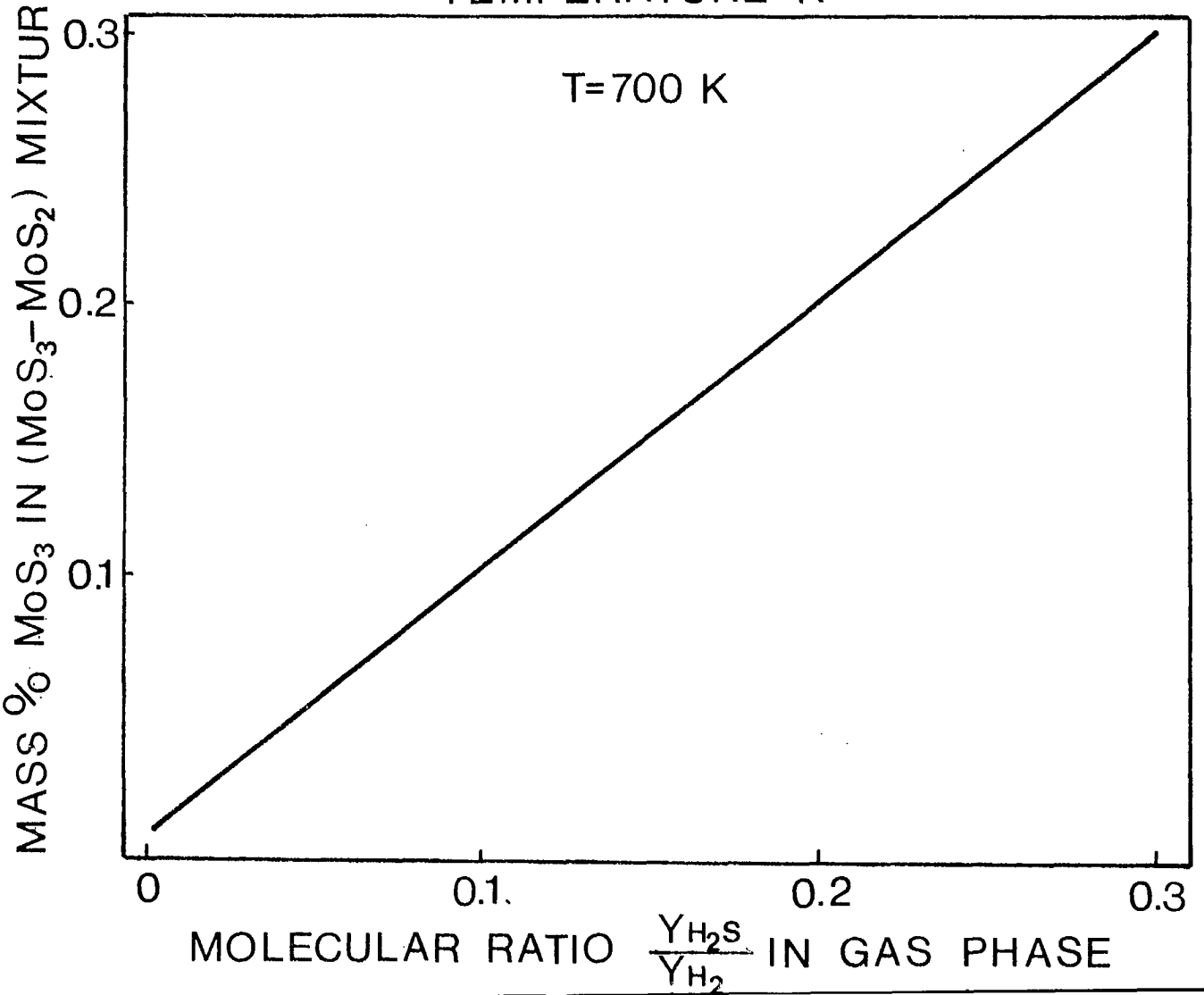
T=700 K
MASS % MoS_3 IN (MoS_3–MoS_2) MIXTURE
0
0.1
0.2
0.3
0
0.1.
0.2
0.3
MOLECULAR RATIO $\frac{Y_{H_2S}}{Y_{H_2}}$ IN GAS PHASE

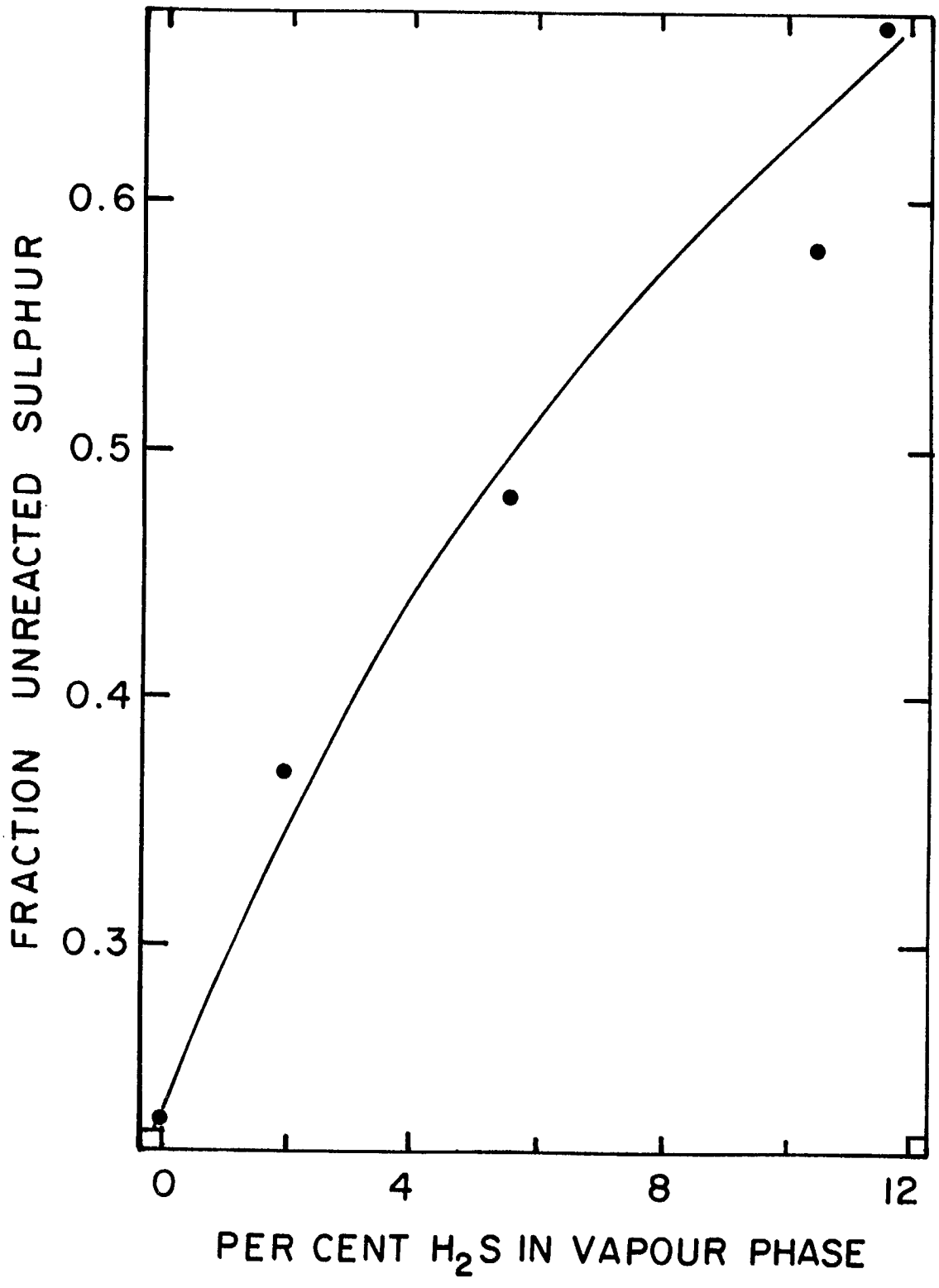
FRACTION UNREACTED SULPHUR
0.6
0.5
0.4
0.3
0
4
8
12
PER CENT H_2S IN VAPOUR PHASE

Fig 7

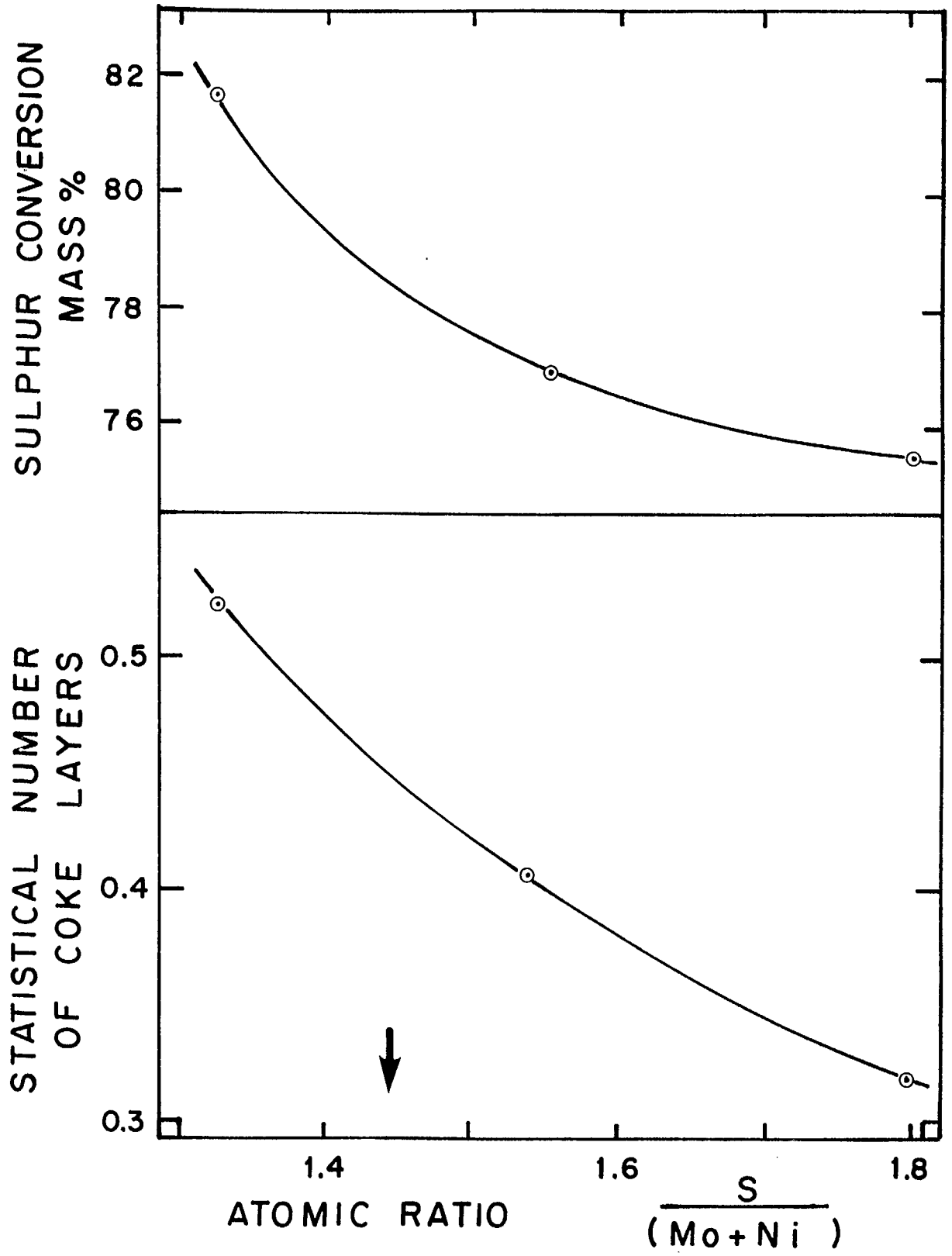
SULPHUR CONVERSION
MASS %
82
80
78
76
STATISTICAL NUMBER
OF COKE LAYERS
0.5
0.4
0.3
1.4
1.6
1.8
ATOMIC RATIO
S
(Mo+Ni)

FIG 8

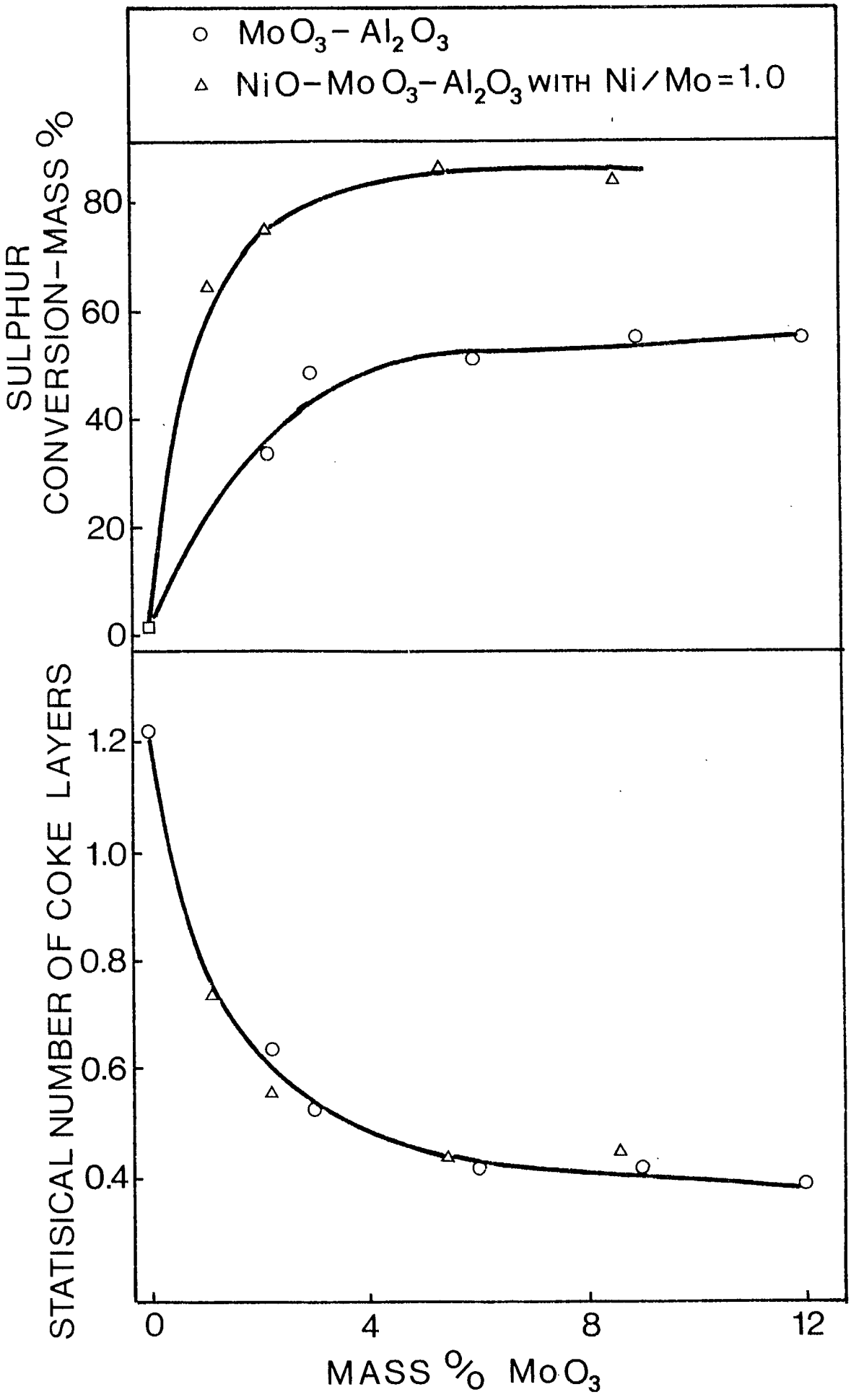
○ $MoO_3-Al_2O_3$
△ $NiO-MoO_3-Al_2O_3$ WITH Ni/Mo=1.0
SULPHUR CONVERSION-MASS %
0
20
40
60
80
STATISICAL NUMBER OF COKE LAYERS
0.4
0.6
0.8
1.0
1.2
0
4
8
12
MASS % MoO_3

Fig 1

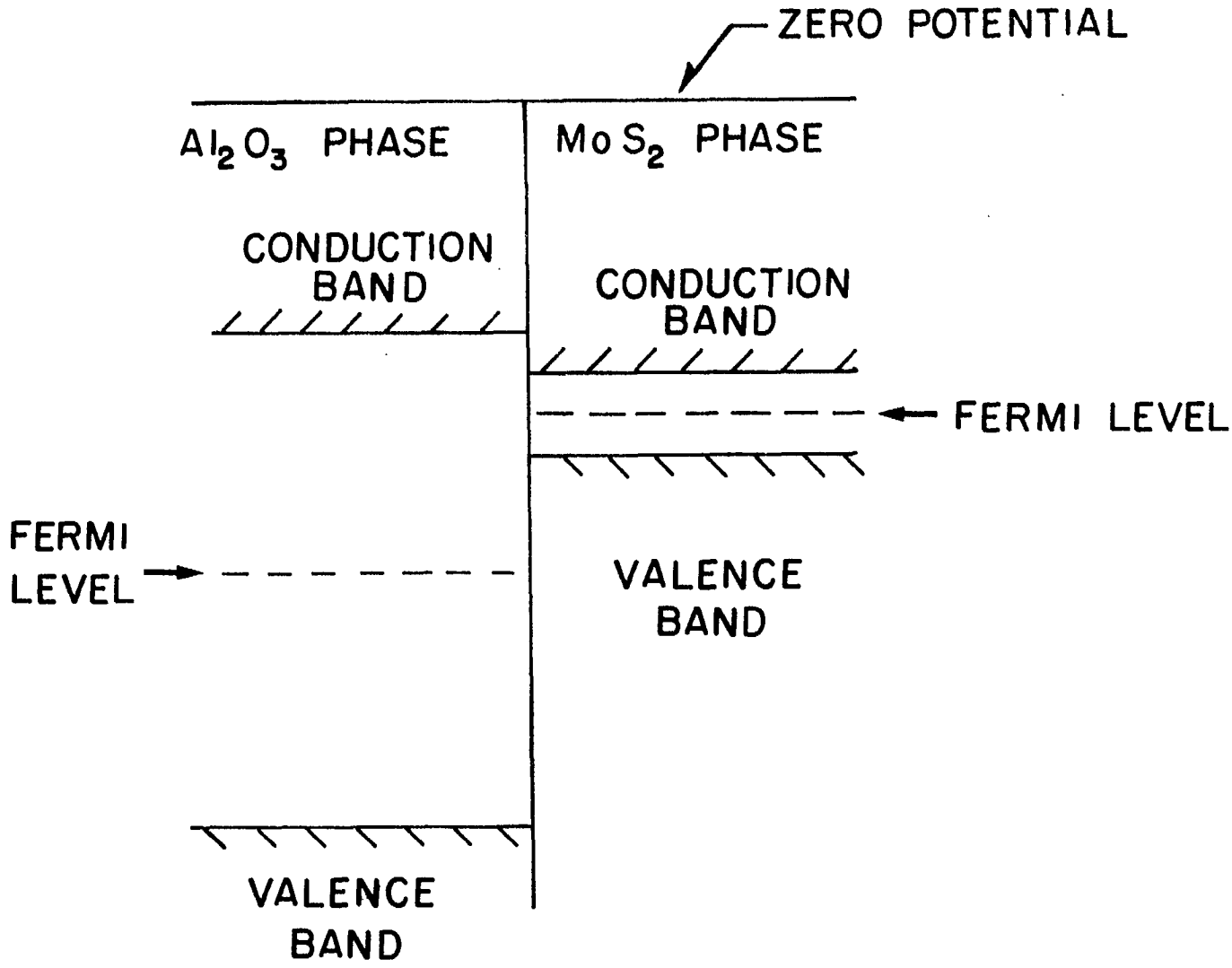
ZERO POTENTIAL
Al_2O_3 PHASE
MoS_2 PHASE
CONDUCTION BAND
CONDUCTION BAND
FERMI LEVEL
FERMI LEVEL
VALENCE BAND
VALENCE BAND

FIG 10

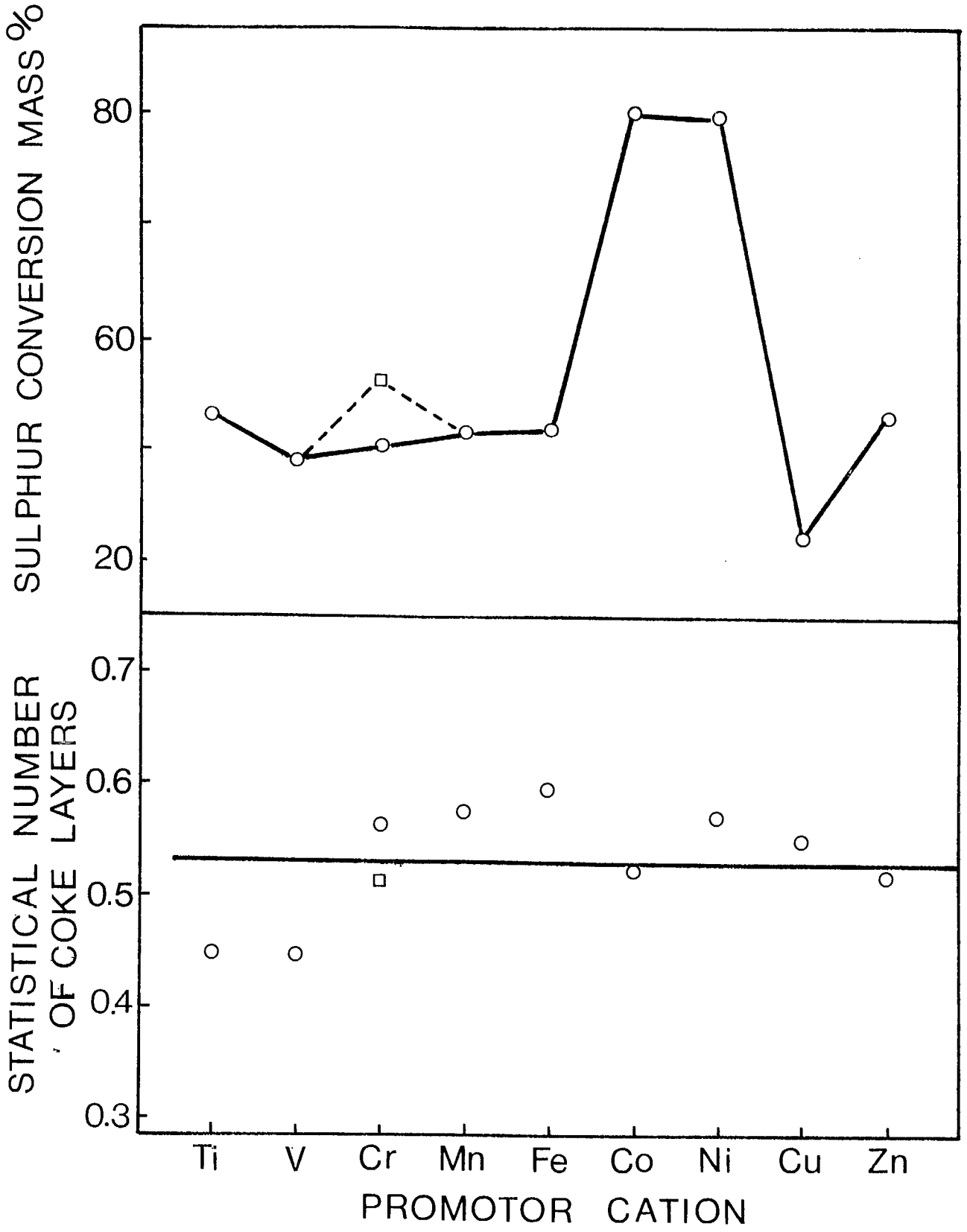
SULPHUR CONVERSION MASS %
80
60
20
STATISTICAL NUMBER OF COKE LAYERS
0.7
0.6
0.5
0.4
0.3
Ti
V
Cr
Mn
Fe
Co
Ni
Cu
Zn
PROMOTOR CATION

FIG 1

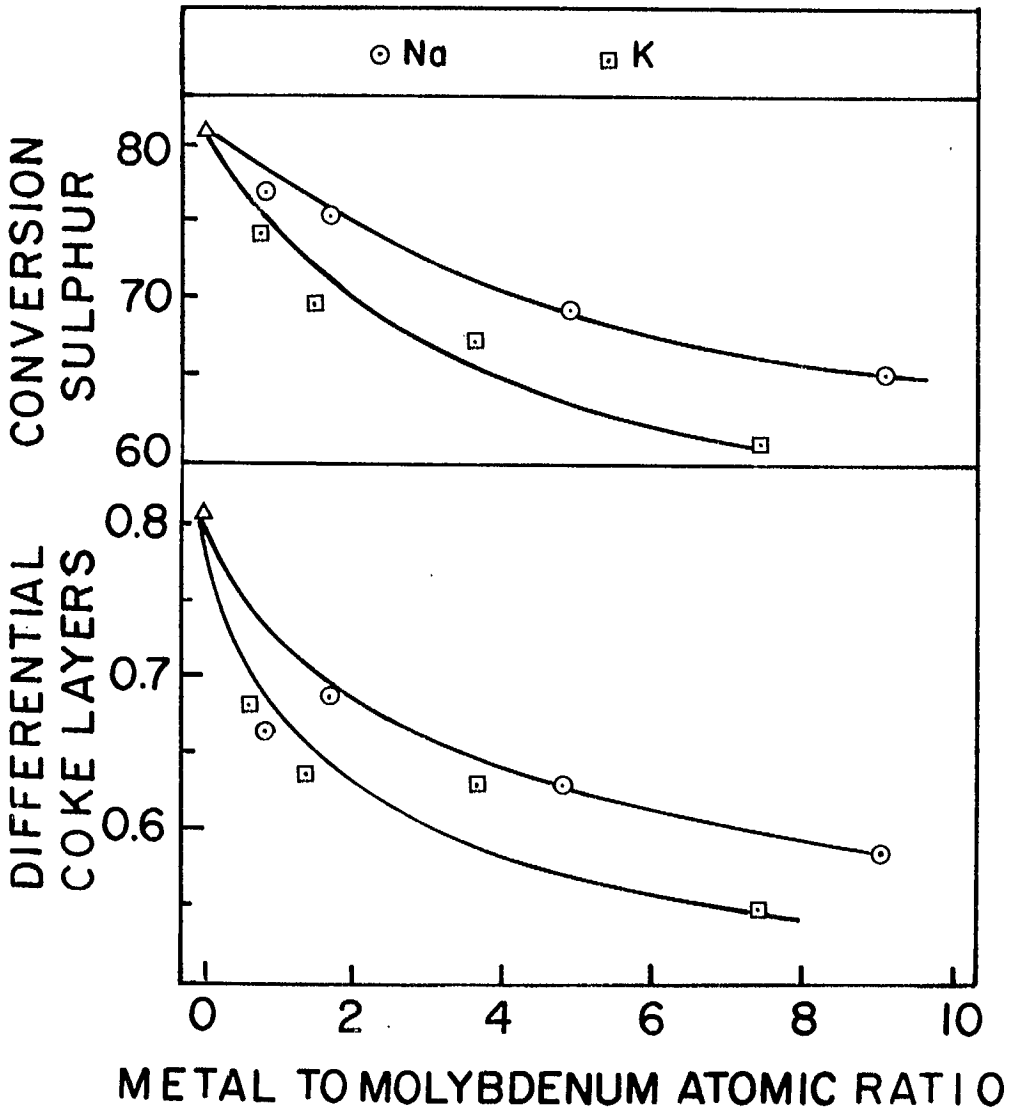
⊙ Na
⊡ K
CONVERSION SULPHUR
80
70
60
DIFFERENTIAL COKE LAYERS
0.8
0.7
0.6
0
2
4
6
8
10
METAL TO MOLYBDENUM ATOMIC RATIO

FIG 1.

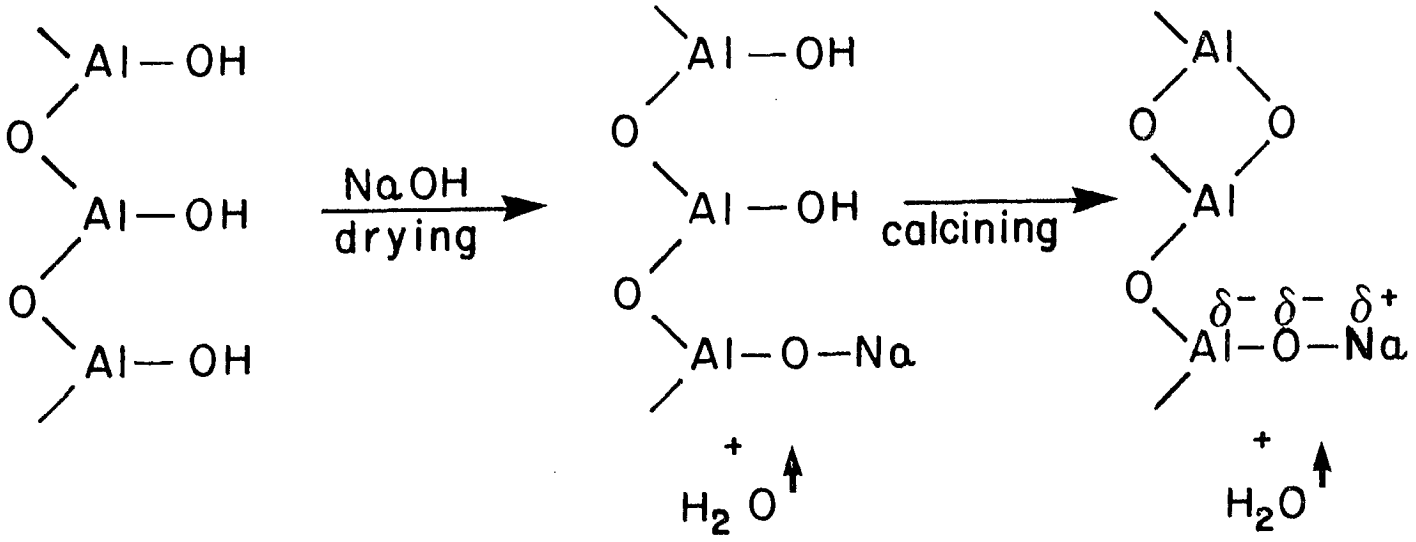
Al—OH
O
Al—OH
O
Al—OH
NaOH
drying
Al—OH
O
Al—OH
O
Al—O—Na
+
H2O
calcining
Al
O
O
Al
O
δ- δ- δ+
Al—O—Na
+
H2O

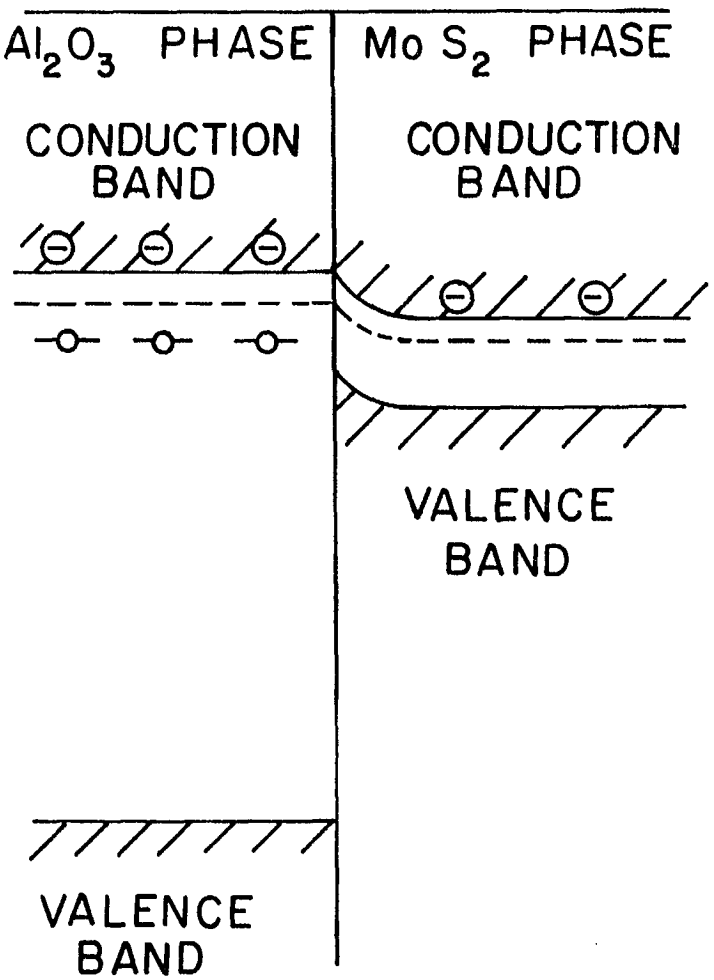
Al2O3 PHASE
Mo S2 PHASE
CONDUCTION BAND
CONDUCTION BAND
VALENCE BAND
VALENCE BAND

Fig 13

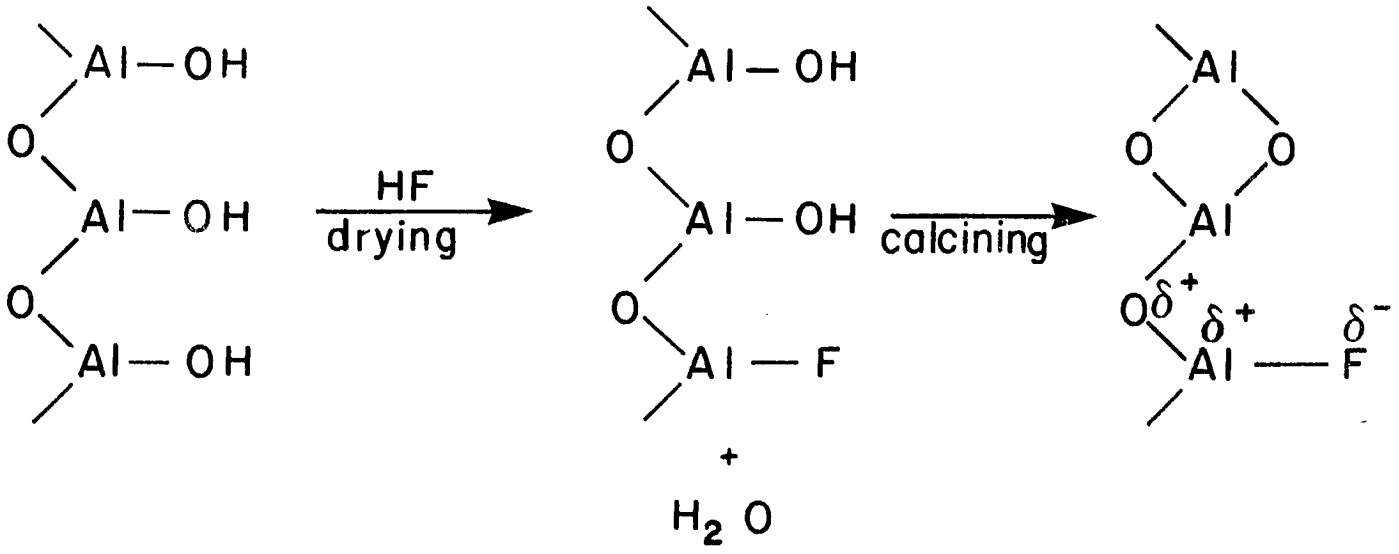
Al—OH
O
Al—OH
O
Al—OH
HF
drying
Al—OH
O
Al—OH
O
Al—F
+
H_2O
calcining
Al
O
O
Al
$O^{\delta+}$
$\delta+$
$\delta-$
Al — F

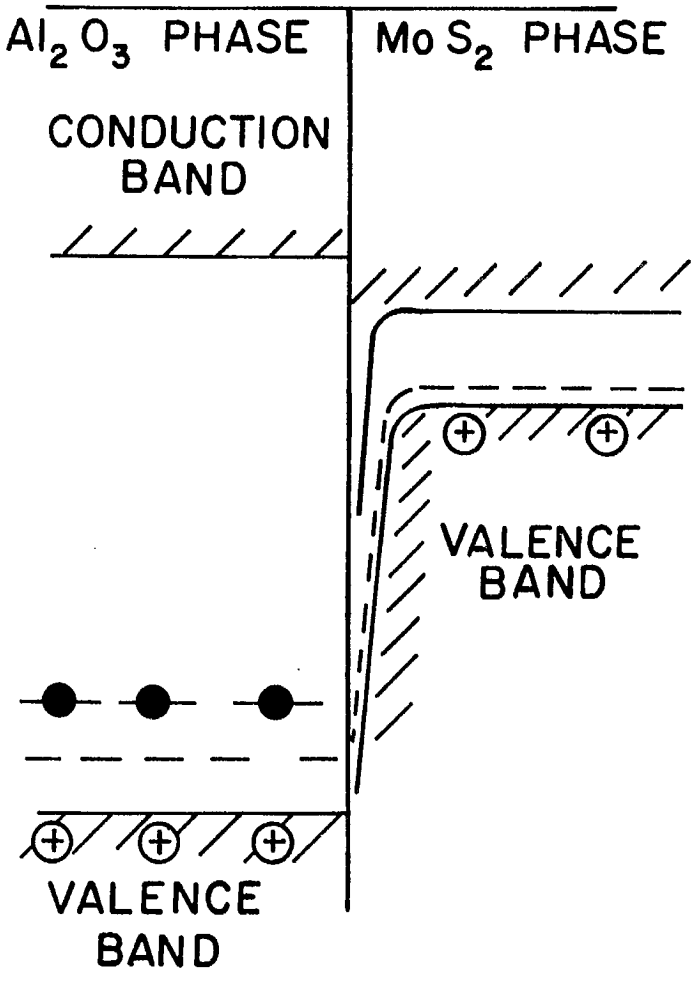
Al_2O_3 PHASE
MoS_2 PHASE
CONDUCTION BAND
VALENCE BAND
VALENCE BAND

Fig 14

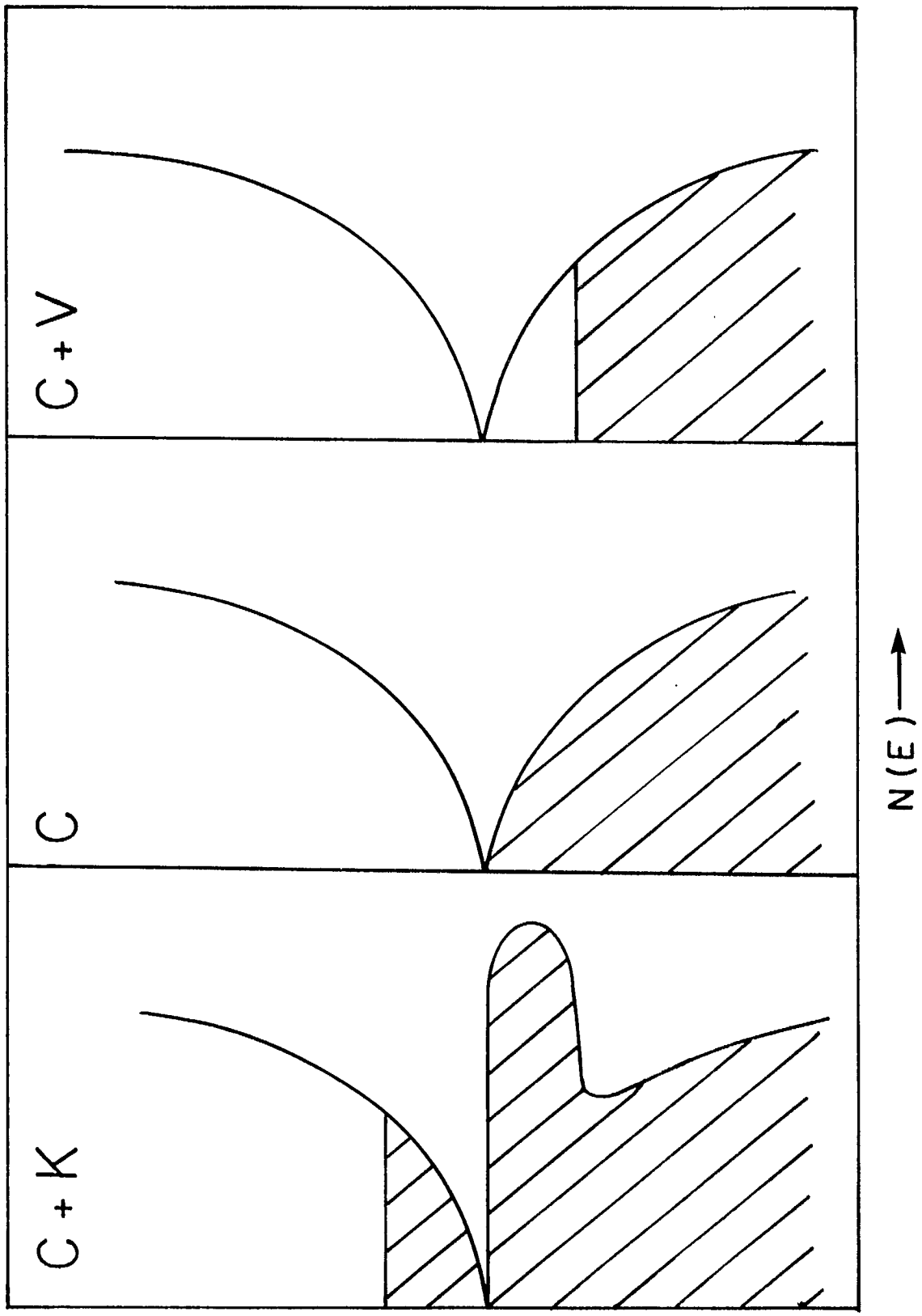

FIG 15

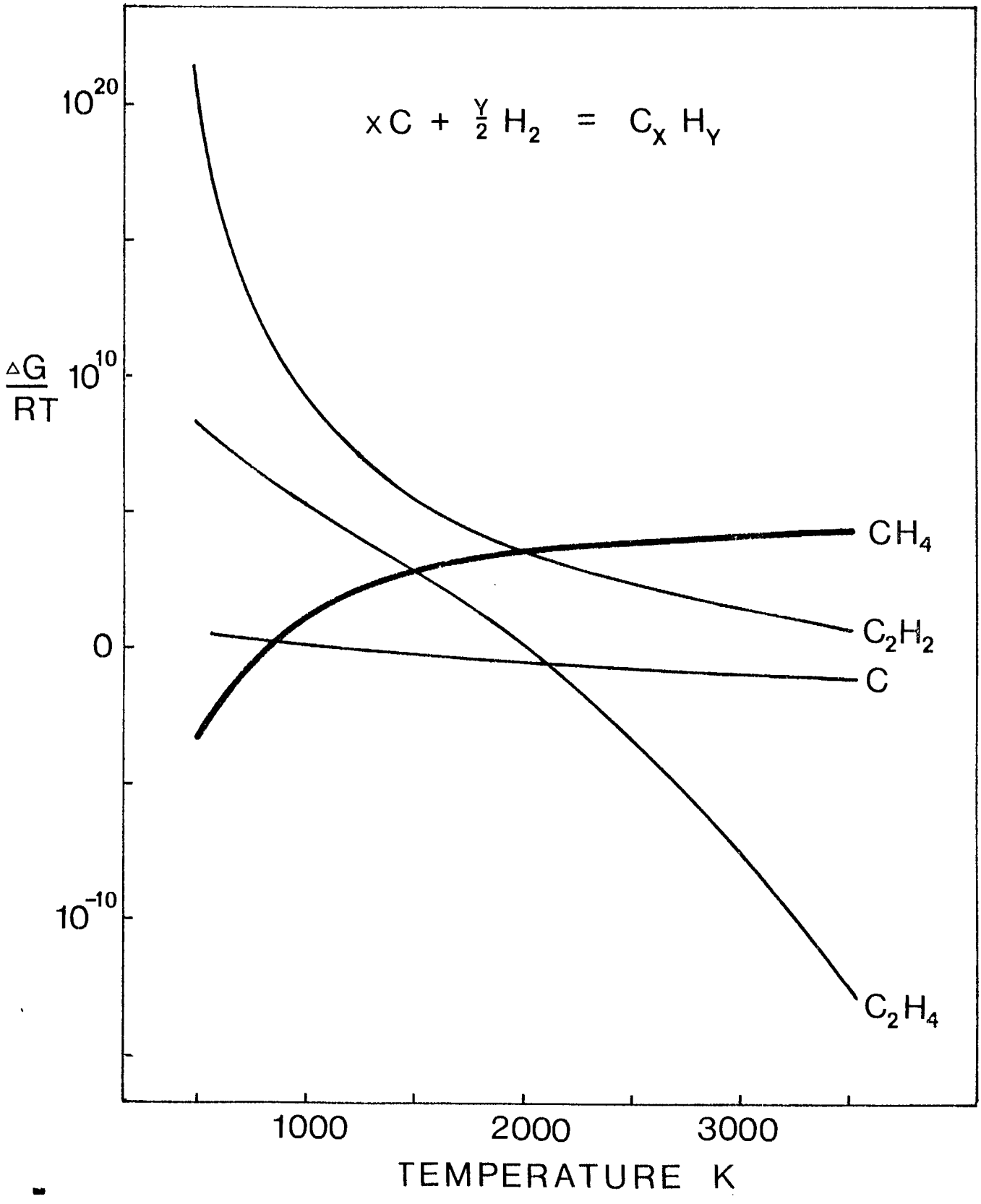
$xC + \frac{Y}{2} H_2 = C_X H_Y$
10^{20}
$\frac{\Delta G}{RT}$ 10^{10}
0
10^{-10}
CH_4
C_2H_2
C
C_2H_4
1000
2000
3000
TEMPERATURE K

FIG 16

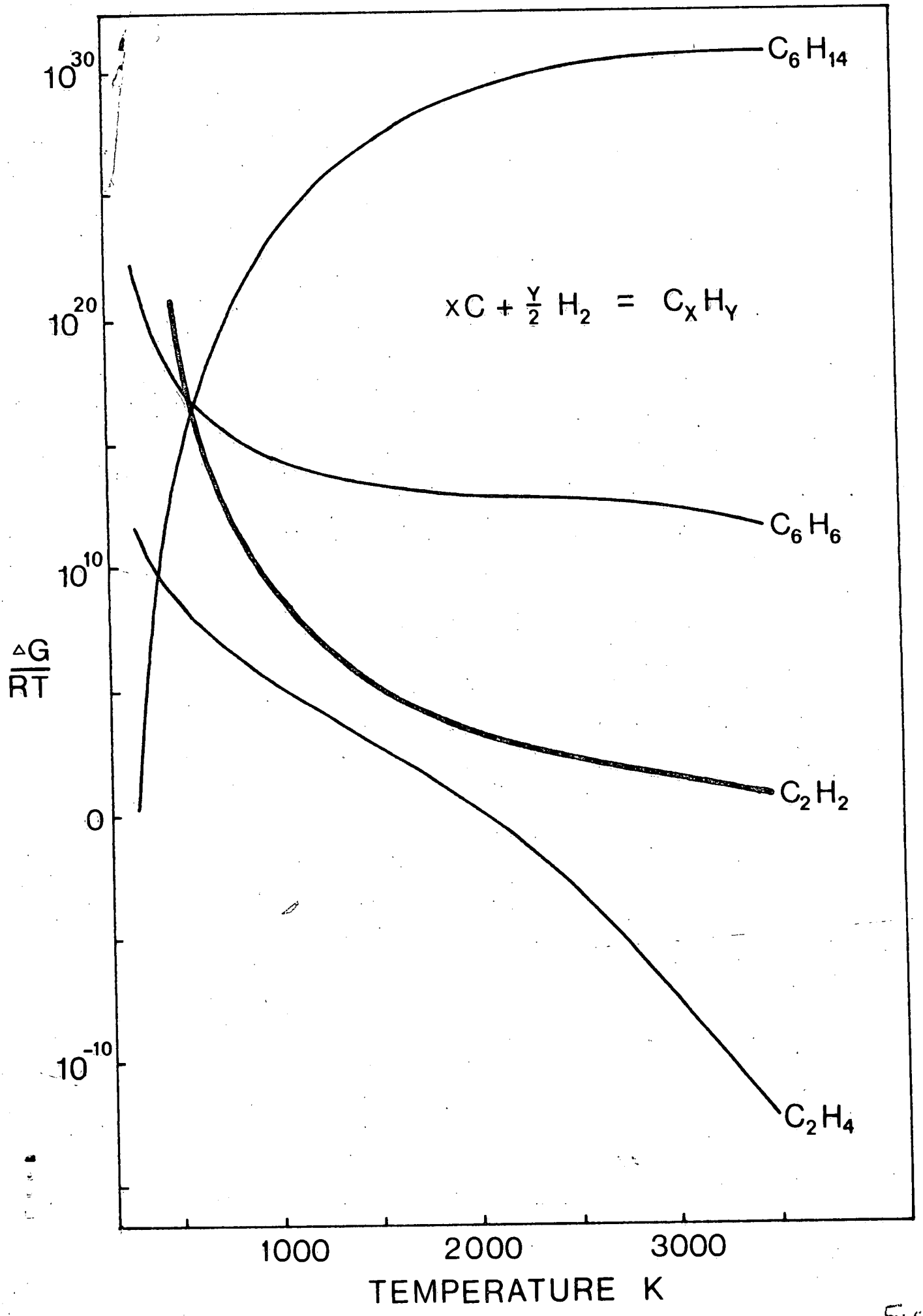
C_6H_{14}
$xC + \frac{Y}{2} H_2 = C_XH_Y$
C_6H_6
C_2H_2
C_2H_4
10^{30}
10^{20}
10^{10}
0
10^{-10}
$\frac{\Delta G}{RT}$
1000
2000
3000
TEMPERATURE K

FIG 17